

FINAL REPORT

THEORETICAL AND EXPERIMENTAL INVESTIGATION OF
TELESCOPIC TUBES IN SIMULATED SOLUTION MINING

by

George L. Smith
Assistant Civil Engineer

Civil Engineering Section
Colorado State University
Fort Collins, Colorado

March 1966

CER66GLS16

INTRODUCTORY REMARKS

This is the final report on the research project "Development of Telescoping Tubes for Use in Solution Mining" .

The main objectives of this research project were to design, construct and test a set of telescoping tubes with a reactive head at the discharge outlet. The telescoping tubes to have an O. D. range from 1-inch (minimum) to 4-inch (maximum) diameter, and to be investigated under various conditions of discharge and buoyancy.

This final report contains three parts. The content of each of them was considered a necessary investigation or activity for the pursual of the research objectives. These three parts are as follows:

- I. STRUCTURAL ANALYSIS
- II. DESIGN AND CONSTRUCTION OF TELESCOPIC JOINTS
- III. HEAD LOSS IN TELESCOPIC JOINTS

Part I refers to the main objective of determining the effect of buoyancy on the performance of telescopic tubes. The original plan of experimental investigation was rejected in favor of a theoretical study, since, by theoretical methods and use of the electronic digital computer, it would be possible to investigate more efficiently

and economically buoyancy effects on telescopic tubes under very wide range of simulated field conditions. The theoretical study using the structural strength of the tube metal as a basis of analysis consisted of the following: (a) the determination of the maximum possible length of nested telescopic tubes for a given diameter range; and (b) the determination of the maximum possible deflection of the length of the nested tubes determined in (a) . The degree of deflection would be the measure of the performance of the various lengths of nested tubes as a function of buoyancy.

Part II refers to the main objective of developing connecting joints between various sections of tubes of different diameters. The joint was to provide for the following: (a) a minimum clearance between the outside and inside diameters of the nested tubes as it would effect total length; (b) a leak proof connection between adjoining tubes; and (c) freedom of lateral movement of the nested tubes from full extension to full contraction. The development of the final design was accomplished largely by trial and error methods by the shop personnel, under the supervision of myself and the shop foreman, Mr. Ralph Asmus.

Part III refers to the main objective of determining the hydraulics of the flow through the nested tubes. This consisted essentially of experimental investigation of the energy loss for

steady flow through the tubes. Besides the loss produced by flow through the tubes, the energy loss produced by the telescopic joints was also investigated. The losses were then related to various flow characteristics and tube geometry for possible field use.

Dr. Albert H. Barnes and Dr. Vujica M. Yevdjevich acted as consultants in the investigations of this report.

Principal Investigator



George L. Smith
Assistant Professor

TABLE OF CONTENTS

<u>Chapter</u>	<u>Page</u>
I. STRUCTURAL ANALYSIS	1
A. INTRODUCTION.....	1
B. EFFECT OF SPECIFIC GRAVITY AND ALLOWABLE STRESS ON LENGTH.....	1
1. Theory.....	1
2. Data Analysis.....	4
3. Discussion	6
4. Conclusions	10
C. EFFECT OF SPECIFIC GRAVITY AND ALLOWABLE STRESS ON DEFLECTION.....	11
1. Theory.....	11
2. Data Analysis	14
3. Discussion	15
4. Conclusions	16
II. DESIGN AND CONSTRUCTION OF TELESCOPIC JOINTS.....	18
A. TYPES OF TUBES	18
B. TYPES OF TELESCOPIC JOINTS	18
1. Lock Joint	19
2. Slip Joint	19

TABLE OF CONTENTS - continued

<u>Chapter</u>	<u>Page</u>
C. TESTING OF SLIP JOINT	21
D. DESIGN RECOMMENDATIONS	23
III. HEAD LOSS IN TELESCOPIC TUBES	25
A. THEORY	25
B. EXPERIMENTAL INVESTIGATION	29
C. CONCLUSIONS	30

LIST OF FIGURES AND PLATES

<u>Figure</u>	<u>Page</u>
1. Cantilever beam with effective uniform, w_e , per unit of length	31
2. Geometric characteristics of the tube with a = specific gravity	31
3. Length of telescopic aluminum tube as a function of specific gravity of the salt brine (Specific gravity tube = 2.70; σ = 14, 000 psi)	32
4. Length of telescopic stainless steel tube as a function of specific gravity of the salt brine (Specific gravity tube = 7.80; σ = 20, 000 psi)	33
5. Minimum diameter (O. D.) at which telescopic aluminum tubes conveying water for solution mining will float for given specific gravity of salt brine (Specific gravity of tube = 270; σ = 14, 000 psi).....	34
6. Relation between minimum diameter of tele- scopic aluminum tubes and total length for various specific gravities of brine (Specific gravity tube = 2.70; σ = 14, 000 psi)	35
7. Relation between minimum diameter of tele- scopic stainless steel tubes and total length for various specific gravities of brine (Specific gravity tube = 7.80; σ = 20, 000 psi)	36
8. Area moments for any point on a uniformly loaded cantilever beam	31
9. Cross-section of a uniformly loaded cantilever beam.....	31
10. Area moments for a cantilever variously loaded with w_n load per unit length	37

LIST OF FIGURES AND PLATES - continued

<u>Figures</u>		<u>Page</u>
11.	Deflection of aluminum telescopic tubing for various densities of salt brine (Specific gravity tube = 2.70)	38
12.	Deflection for given total length of aluminum telescopic tubing for various densities of salt brine (Specific gravity tube = 2.70)	39
13.	Deflection of stainless steel tubing for various densities of salt brine (Specific gravity tube = 7.80)	40
14.	Deflection for given total length of stainless steel tubing for various densities of salt brine (Specific gravity tube = 7.80)	41
15.	Sudden contraction in a pipe line	42
16.	Variation of resistance coefficient for uniform flow in aluminum tubes as compared with the moody resistance diagram	43
17.	Variation of telescopic joint energy loss coefficient with Reynolds number for various ratios of tube diameters	44
<u>Plates</u>		
1.	Preliminary design of telescoping tube lock joint	45
2.	Final design of telescoping tube slip joint showing details of joint with all tubes in extended position	46
3.	Details of telescoping tube slip joint not shown in Plate 2	47
4.	Discharge system for extension or contraction of telescopic tubes	48
5.	Schematic view showing various energy lines and method of determining head loss along the telescopic tube and at the telescopic joints	49

I. STRUCTURAL ANALYSIS

A. INTRODUCTION

The basic problem to be solved by this section of the report is to determine the theoretical maximum length and deflection of a set of nested telescopic tubes of a given range of diameters as a function of specific gravity of pumped fluid, tube material and brine concentration. The solution will consist of two parts, namely: (a) the determination of the maximum length of n sections of tube on the basis of the structural strength of the tube material only, and (b) the determination of the maximum deflections of those maximum lengths of n sections of tube determined in part (a) .

B. EFFECT OF SPECIFIC GRAVITY AND ALLOWABLE STRESS ON LENGTH

1. Theory

The n -th telescopic tube from the end will be considered as a cantilever beam uniformly loaded, as illustrated in Figure 1 . The theory relates to telescopic tubes which are freely extended into the brine, and which do not touch or lean on the bottom of dissolving salt ore.

From Figure 1 the following expression is obtained

$$M_n - \frac{w_{e_n} L_n^2}{2} - W_o L_n - M_{n-1} = 0 \quad (1)$$

in which M_n is the maximum moment at the left support equal to σS , with σ the allowable unit stress at the outer fiber. For aluminum σ is taken as 14,000 psi; for stainless steel it is taken as 20,000 psi. S is the strength modulus of the section. The expression $\frac{w_{e_n} L_n^2}{2}$ is equal to the force $w_{e_n} L_n$ produced by a uniformly loaded cantilever beam acting at a distance $\frac{L}{2}$ from the point of support. $W_o L_n$ is the moment of a single force, W_o , equal to the weight of n continuous cantilevered tubes to the right of W_o , as given in Figure 1 of varying uniform weight, w_e . M_{n-1} is the maximum moment developed at the extreme right end of the n -th section of telescopic tube.

Equation 1 is now defined in terms of the geometry of the telescopic tubes and the specific gravities of the tube material, pumped fluid and the brine concentration. From Figure 2 the following expressions are obtained:

Area of outside diameter

$$A_o = \frac{\pi}{4} D^2 \quad (2)$$

Area of inside diameter

$$A_i = \frac{\pi}{4} (D - 2t)^2 \quad (3)$$

Cross-section area of the tube

$$A_p = A_o - A_i = \frac{\pi}{4} [D^2 - (D - 2t)^2] = \frac{\pi}{4} (4Dt - 4t^2) \quad (4)$$

The equation for effective uniform load, weight w_e , in terms of tube geometry and specific gravities of tube material, pumped fluid and brine concentration becomes

$$\begin{aligned} w_e &= \gamma (A_p \alpha_t + A_i \alpha_w - A_o \alpha_b) \\ &= 62.4 \left[\frac{\pi}{4} (4Dt - 4t^2) \alpha_t + \frac{\pi}{4} (D - 2t)^2 \alpha_w - \frac{\pi}{4} (D^2) \alpha_b \right] \end{aligned} \quad (5)$$

in which α_t is the specific gravity of the tube material,

α_w is the specific gravity of the pumped water taken as 1.0, and

α_b is the specific gravity of the brine concentration produced by the solution mining.

Equation 5 can be further simplified to

$$w_e = 15.6\pi [D^2 (\alpha_t - \alpha_b) - (D - 2t)^2 (\alpha_t - 1.0)] \quad (6)$$

Converting w_e to pounds per inch divide by 1728 gives

$$w_e = 0.0284 [D^2 (\alpha_t - \alpha_b) - (D - 2t)^2 (\alpha_t - 1.0)] \quad (7)$$

The expression for S in terms of tube geometry is

$$S = \frac{\pi}{32} \frac{(D^4 - D_i^4)}{D} \quad (8)$$

With

$$(D^4 - D_i^4) = (D^2 + D_i^2) (D + D_i) (D - D_i) \quad (9)$$

Since $D_i = D - 2t$, Eq. 10 can be written as

$$(D^4 - D_i^4) = 8(D^2 - 2Dt + 2t^2) (D - t) (t) \quad (10)$$

Substituting Eq. 10 into Eq. 8 gives

$$S = 0.7854 \frac{(D^2 - 2Dt + 2t^2) (D - t) (t)}{D} \quad (11)$$

2. Data Analysis

To determine the maximum length of telescopic tube, the following tube geometry and specific gravities of tube and brine concentration were considered.

$$D_{\min} \text{ (O.D.)} = 0.5 \text{ inch}$$

$$D_{\max} \text{ (O.D.)} = 4.0 \text{ inch}$$

$$t = \text{constant} = 0.065 \text{ inch}$$

$$\alpha_b = 1.00, 1.05, 1.10, 1.15 \text{ and } 1.20$$

$$\alpha_t = 2.70 \text{ (aluminum); } 7.80 \text{ (stainless steel)}$$

$$\alpha_w = \text{constant} = 1.00 .$$

Thus the clearance between the inside diameter and outside diameter of all nested tubes is taken to be a constant value of 0.125 inch or 0.065 inch on a side. (See Section II, Telescopic Tube Joints for further details). Two types of metal tubes only were selected for analysis, namely: (a) aluminum tubes, and (b) stainless steel tubes. The two metals were selected on the basis that their specific gravities represent the minimum and maximum range of tubes available on the commercial market. Aluminum tubing was used in laboratory studies of telescopic tube performance. Furthermore, it has the advantage over stainless steel or other metals in that it is more economical, and has a low specific gravity and therefore is easier to handle. Stainless steel tubing has the advantage of being highly resistant to the corrosive action of the brine, which reacts adversely with aluminum tubing.

In the following analysis, outside of chemical reaction between metal and brine solution, consideration is given to the structural response only of tubes of low and high specific gravity submerged in the brine of various densities. The specific problem to be solved is to determine the maximum possible length of telescopic tubes of a given structural strength and diameter range submerged in fluid of given densities, with several densities investigated. For given tube geometry, specific gravities of the metal tubing, and various specific gravities of the brine solution, use was made of the electronic digital

computer to determine the following:

- a. The maximum length of telescopic tubes of a given metal, which discharges water, as a function of the resultant buoyancy force produced by an increase in specific gravity of the mined salt solution.
- b. The maximum length of telescopic tubes for the conditions of item 1 in which the diameter of the minimum size tube only is increased, i. e., total telescopic length of 1/2-inch - 4-inch set as compared to 3/4-inch - 4-inch set of nested tubes.

3. Discussion

Results obtained by means of the computer program are summarized in Figures 3 through 7. A description and significance of each figure is given in the following paragraphs.

Figures 3 and 4 illustrate the effect of an increase in the specific gravity of the salt brine produced by the solution mining process on total length of telescopic tubes of a given diameter range. The diameter range of the tubes is from 1/2 inch (minimum) to 4 inches (maximum) . Figure 3 is for the aluminum tubes and Figure 4 is for the stainless steel tubes. From an examination of the graphs the following points relative to their use in the field should be noted:

- a. Figure 3, Aluminum tubes:

- (1) Each value on the ordinate of graph 3 , as well as for graphs 4, 6, and 7, gives the incremental increase in

the diameter range of the telescopic tubing. Each value on the abscissa gives the total theoretical length of the given set of telescopic tubes for a given specific gravity of the brine. For Example, the value 0-5-1.5 inches is for a set of nested tubes having the following diameters: 0.5, 0.75, 1.00, 1.25, and 1.50 inches. If the brine solution has a specific gravity of 1.00, the total theoretical length for this set of tubes, from Figure 3, would be 50 feet.

(2) For the specific gravity of the brine solution 1.15 the tubes having a diameter greater than 2.75 inches will float.

(3) An increase in specific gravity of the brine from 1.15 to 1.20 causes a significant reduction in diameter at which the tube will float, i.e., reduction from 2.75 inches to 2.00 inches.

b. Figure 4, Stainless steel tubes:

(1) A 20 percent - 1.00 to 1.20 - increase in specific gravity of brine increases the total length of tubes only 2.2 percent - 61.05 feet to 67.39 feet. There is an apparent finite limit to the total length of stainless steel tubing at saturated conditions of the brine solution.

(2) For an assumed mining operation of specific gravity of brine of 1.10 (170 grams* per liter, 1.4 lbs per gallon) , the lateral radius of the salt cavity could be approximately doubled by using aluminum rather than stainless steel tubing.

For aluminum tubing, the diameter at which flotation occurs at various specific gravity of brine solution is given in Figure 5 . The important point of this figure is that as a saturated condition in the brine solution is approached the curve tends to become asymptotic to approximately 1-inch diameter tubing. Obviously, for anticipated saturated conditions and maximum length of telescopic tubing, the minimum diameter of aluminum tube should not be less than 1 inch.

The effect of increasing the minimum size of the telescopic tubes with range in diameter from 1/2-inch to 4-inches is shown in Figures 6 and 7 for aluminum and stainless steel, respectively. Figure 6 reflects the effect of increased tube diameter of aluminum to flotation. Thus, for a specific gravity of brine of 1.10 , the maximum length of telescopic tubing varies from 131 feet for 1/2-inch to 4-inch range, to 110 feet for the 2-1/4 inch to 4-inch range, and to 195 feet for a single 4-inch diameter pipe. For stainless steel tubing, the variation for a specific gravity of brine of 1.20 is from 67.5 feet (1/2-inch to 4-inch diameter) to 45 feet for single 4-inch diameter

* Handbook of Chemistry and Physics, 44th Edition, 1962, p.2057

tube. In summary, for aluminum tubing the maximum possible length is extremely variable for specific gravities of the brine greater than 1.05; for stainless steel the effect of increasing specific gravity of brine on length is insignificant with an estimated maximum length of telescopic tubes - 1-inch to 4-inch diameter range - of 70 feet.

In reference to Figure 5 , as the specific gravity of the brine increases, the diameter of aluminum tubing at which flotation occurs decreases. The significance of the fact that tubing floats or is too long concerns the lateral movement in solution mining of a given diameter range of telescopic tubes. Their extension or contraction, in general, will not be impeded so long as the developing cavity remains small both in height and in diameter, in other words, so long as the extended tubes lie along the bottom of the salt cavity in essentially a horizontal position. However, as the cavity increases in diameter and height, the larger diameter tubes displacing a greater volume for a given specific gravity will have a greater buoyancy force than a weight force and will tend to rise or float; whereas, the smaller diameter tubes with a greater weight component than buoyancy force will tend to sink resulting in bending or deflection, if they are not supported by the bed. The division point - tube diameter - between these two conditions varying with brine density will be a critical point at which the deflecting tubes will tend to bind and resist further extension. Increased resistance created by

the bending between the floating and deflected tubes will require increased pressure which must be carefully controlled to avoid sudden movement resulting in sharp impact on the joints all along the extended tube sections. Since the joints are points of greatest weakness, a sufficiently sharp impact could cause separation of the tube sections.

Deflection of the smaller diameter tubes can be minimized by use of the impulse-momentum principle in which jets of sufficient number issuing from port holes along the bottom of the tubes will cause the tubes to float. Obviously, discharge used in producing flotation must be subtracted from the discharge needed for solution mining ahead of the telescopic tubing. Further consideration of telescopic tubes with manifold flow through orifices along the tube sections is beyond the scope of this report.

4. Conclusions

From this analysis of effect of specific gravity and allowable stress on length of telescopic tubes, the following pertinent points are to be noted:

- a. If properly protected from action of the salt brine, the aluminum tubes will provide the greatest telescopic length of metal tubing available on the commercial market.
- b. For maximum length of telescopic tubing, assuming an average brine density of 1.20 during mining operation, the

minimum diameter of aluminum tubing should not be less than 2 inches (See Figure 6) .

c. The 2-inch diameter limit for aluminum tubing will minimize:

(1) effect of deflection on contraction and extension of tubes, and

(2) need for pipe stability in the horizontal plane by jet flow from bottom port holes along the tube, and thus increase scouring ability at discharge head.

d. For stainless steel tubing, and increase of 20 percent in specific gravity of brine will increase total length only 10 percent. The maximum total length would not exceed 100 feet at 50 percent saturation. (Specific Gravity of brine = 1.20)

C. EFFECT OF SPECIFIC GRAVITY AND ALLOWABLE STRESS ON DEFLECTION

1. Theory

If two vertical sections are taken through the beam of Figure 8, the free body of Figure 9 may be obtained. Since the body is in equilibrium under the action of the load and the internal forces, the moment taken about the right side of the element can be expressed in terms of the moment and shear on the left side and the intervening loads, or

$$M_x = M + V_x - \frac{wx^2}{2} \quad (12)$$

Let A in Figure 8 be an origin where the moment and shear are known.

$$M_A = -\frac{wa^2}{2} ; \quad V_a = -wa$$

$$M_B = -\frac{wa^2}{2} - wax - \frac{wx^2}{2} \quad (13)$$

The slope at any point on the moment curve is $dM/dx = V$, and hence the area of the moment diagram between A and B can be divided into a rectangle, a triangle whose hypotenuse is tangent to the curve, and a parabolic area.

For the purpose of analysis, the telescopic pipes will be considered as a cantilever beam variously loaded with different weights, w , per unit length. (See Figure 10) Furthermore, with the change of unit weight being a function of the given cross-sectional geometry of the telescopic pipes, the deflection of the pipes between any two points will be determined by the area moment method. The method makes use of the following axiom: "The area of the moment diagram between any two points is equal to EI times the change in slope of the elastic curve between those two points". E is the modulus of elasticity and I is the moment of inertia.

Taking moments about A of the area between C and D in Figure 10 gives the deflection between C and D, or

$$\begin{aligned}
-EI_3 \Delta y_3 &= \left(\frac{w_1 L_1^2}{2} + w_1 L_1 L_2 + \frac{w_2 L_2^2}{2} \right) (L_1 + L_2 + \frac{1}{2} L_3) (L_3) \\
&+ (w_1 L_1 + w_2 L_2) (L_3) \left(\frac{1}{2} \right) (L_3) (L_1 + L_2 + \frac{2}{3} L_3) \\
&+ \left(\frac{w_3 L_3^2}{2} \right) \left(\frac{1}{3} \right) (L_3) (L_1 + L_2 + \frac{3}{4} L_3) \quad (14)
\end{aligned}$$

The total deflection is the sum of the individual deflections produced by the moments of the individual areas, AB, BC, and CD, or

$$y_T = \Delta y_1 + \Delta y_2 + \Delta y_3 + \dots + \Delta y_n \quad (15)$$

To determine the total deflection, Equation 15 can be generalized as follows:

$$\begin{aligned}
-\Delta y_n &= \frac{L_n}{EI_n} \left\{ \left[\sum_{i=1}^{n-1} \frac{w_i L_i^2}{2} + \sum_{i=2}^n (L_i \sum_{j=1}^{i-1} w_j L_j) \right] \left[\sum_{i=1}^{n-1} L_i + \frac{L_n}{2} \right] \right. \\
&+ \left[\frac{L_n}{2} \sum_{i=1}^{n-1} w_i L_i \right] \left[\sum_{i=1}^{n-1} L_i + \frac{2}{3} L_n \right] \\
&\left. + \left[\frac{1}{6} w_n L_n^2 \right] \left[\sum_{i=1}^{n-1} L_i + \frac{3}{4} L_n \right] \right\} \quad (16)
\end{aligned}$$

The total deflection is equal to

$$-y_T = \sum_{n=1}^m \Delta y_n \quad (17)$$

2. Data Analysis

As for the determination of the theoretical total length, the analysis of deflection was made using the electronic digital computer. Furthermore, the theoretical maximum lengths as previously determined were used in the following analysis. Standard lengths available on the commercial market were not considered. The purpose of this analysis being to determine the theoretical upper limit of deflection for a given set of conditions of the telescopic tubes as follows:

- a. The range in diameter of the nested telescopic tubes was from a minimum diameter of 1 inch to a maximum diameter of 4 inches.
- b. The range in specific gravity of brine was from 1:00 to 1:20 .
- c. The two types of tubes considered were aluminum tube of specific gravity 2.70 , and stainless steel tube of specific gravity of 7.80 .

3. Discussion

The results of the analysis are given in Figures 11 through 14 . Figures 11 and 12 are for aluminum tubing; Figures 13 and 14 are for stainless steel tubing.

Figures 11 and 13 show the effect of increasing the density of the salt brine on total length and deflection of the telescopic tubes. Figure 11 , for example, if the diameter range of the nested telescopic aluminum tubing were 1 - 3.50 inches, its total length in a brine solution having a specific gravity of 1.00 would be 82.5 feet. If the specific gravity of the brine was increased from 1.00 to 1.05 (5% increase) , the total length would be increased 8.8 feet to 91.3 feet (10.68% increase) . The total deflection of the 82.5 feet of 1 - 3.5 inch telescopic tubing would be 46 feet. (See Figure 12 also) The increase in length of 8.8 feet would result in an increase in deflection of 9.5 feet as read from Figure 11 . The increase in deflection would be from 46.0 feet to 55.5 feet or a 20% increase. In a similar manner, an analysis can be made of stainless steel tubing from Figure 13 . An analysis for 1 - 3.5 inch diameter of aluminum and stainless steel telescopic tubing is summarized in the following tables:

Table 1 - Effect of Brine Density on Length and Deflection of 1 - 3.5 Inch Aluminum Telescopic Tubing (Sp. Gr. Tube = 2.20)

Percent Increase in Sp. Gr. of Brine	Percent Increase in Tube Length	Percent Increase in Tube Deflection
5	10.68	20.60
10	27.00	55.50
15	Tube floats	Tube floats
20	Tube floats	Tube floats

Table 2 - Effect of Brine Density on Length and Deflection of 1 - 3.5 Inch Stainless Steel Telescopic Tubing (Sp. Gr. Tube = 7.80)

Percent Increase in Sp. Gr. of Brine	Percent Increase in Tube Length	Percent Increase in Tube Deflection
10	4.86	9.35
20	10.60	20.80

Figure 12 gives the total deflection for various total lengths of the telescopic aluminum tubing as a function of the specific gravity of the brine. Each point on each curve is for a given diameter range of telescopic tubing. The maximum range of 1 - 4.00 inches is so indicated. Figure 14 is the same as Figure 12 except that it is for stainless steel.

4. Conclusions

From the analysis of data summarized in Figures 11 through 14, the following conclusions are drawn:

- a. For a given increase of brine density, the rate of increase of total deflection is greater than the rate of increase of total length of telescopic tubing.

- b. On the basis of item 1 , using a lighter tubing such as aluminum does not necessarily mean that the deflection will be less than that of tubing of equal length but of greater specific gravity in a brine of high density.
- c. For stainless steel tubing the ratio of percent increase of tube length to the percent increase of tube deflection seems to occur at a rate of 1:2 .

II. DESIGN AND CONSTRUCTION OF TELESCOPIC JOINTS

A. TYPES OF TUBES

In the design and construction of telescopic tube joints, the two types of tubes investigated were (1) aluminum, and (2) stainless steel. Tubing was selected rather than pipe, because of the need of close tolerance between the inside and outside diameter of the telescopic section in order that a maximum length of telescopic units could be obtained. In regard to the type of metal chosen, aluminum and stainless steel represented the minimum and maximum weight limits of commercially available tubing. It was recognized that aluminum would corrode rapidly in the brine solution, but it was assumed that with various coating materials now available on the market, sufficient protection could be provided for their use in solution mining. Several such lubricants were tested and are discussed in more detail in a later paragraph.

B. TYPES OF TELESCOPIC JOINTS

Two types of telescopic joints were investigated: (1) the lock joint, and (2) the slip joint. Details of the lock joint are shown on Plate 1; details of the slip joint are shown on Plates 2 and 3 .

1. Lock Joint

The lock joint, as the name implies, was designed to hold the telescopic sections in a fixed position after full extension. This precluded the retraction of a section after reaching its terminal position. Objections to this type of joint included:

- a. The inability to contract or expand the telescopic tubes under remote control conditions.
- b. The weakening of joints because of the required grooving for the seal rings.
- c. The difficulty in obtaining seal rings of sufficient elastic strength for desired cross-sectional area. Special made rings of teflon and spring steel were obtained, but found undesirable on a structural basis.
- d. Special tooling and precision machine work required for the grooves for the seal rings.

2. Slip Joint

The slip joint was installed on both stainless steel and aluminum tubing. Essentially, three steps were needed in the development of the final acceptable slip joint. Initially three 20-foot sections of stainless steel tubing with a $1/16$ inch tolerance - $1/32$ inch on a side - were investigated. The minimum diameter was 1 inch . Because the tubes were more ellipisoidal than circular in shape,

the tubes had to be reshaped by polishing and grinding. Besides greatly increasing initial costs, it was found that the tubes tended to bond even after a thorough coating of silicone lubricant. In favor of operation of the nested tubes over desired total length, the tolerance between inside and outside diameter was increased to $1/4$ inch - $1/16$ inch on a side.

After the selection of the $1/4$ -inch tolerance, the slip joint was constructed on three sections of stainless steel tubes of outside diameter of 1 inch, $1-1/4$ inch and $1-1/2$ inch respectively. The joint was designed and constructed for expansion only, although it could be returned to its original position by pushing on the nozzle. The slip joint, as shown in Plates 2 and 3, consisted of the following components:

- a. A $1-1/2$ -inch brass sleeve sweated on and silver soldered into position at the end of each tube section. Tolerance between sleeve and inside diameter of the next larger tube was $1/64$ inch. Also, a rubber O-ring was placed on the sleeve to provide a seal against leakage at the joint.
- b. A series of $1/8$ -inch wide alternating brass and teflon bushings on the end opposite the $1-1/2$ -inch brass sleeve. Three brass and two teflon bushings were used. The bushings served not only as a guide, but also provided a shoulder stop for the brass sleeve of the smaller diameter tube.

For the second step, slip joints were constructed for contiguous aluminum tubing from 1 inch to 3 inches in diameter in which the outside diameter was varied in 1/4-inch increments. The only difference in the construction of the joint for the aluminum tubes was in the method of attachment of the various rings. Great difficulty was encountered in using a brass-aluminum solder for attachment of the brass sleeves, which were available as surplus from the previous investigation of the slip joints involving stainless steel tubing. In lieu of brass-aluminum solder, several epoxy glues were then tried until one having the brand name of Hysol was found to be satisfactory. In this, the second step, interest was in expansion only. Contraction as well as expansion was considered next.

C. TESTING OF SLIP JOINTS

The final step was to simulate field conditions as nearly as possible with the exception of floating the tubes in a brine solution. For this step the tubes were placed in a 10-inch diameter pipe with removable plastic covers near the entrance, middle, and discharge end for observation purposes. With covers in place the ambient pressure surrounding the telescopic tube could be regulated. Also, the 10-inch diameter pipe simulated the cavity which would be developed initially by the tube. For simulating remote control of the tubes a flow control system of discharge and suction was then

attached to the telescopic tubes as shown in Plate 4 . The system consisted of a centrifugal pump, control valves, pipe lines and a pressure gage located on the supply line to the nested tubes.

On the basis of observation of the performance of the tubes, the following modifications of the tube joints were made:

1. To prevent jamming of the tubes on retraction, a 3/8-inch brass collar was attached to the tube by means of metal screws. The collar diameter should be equal to or slightly larger than the next size larger tube.
2. To prevent binding at the joints, it was necessary to increase the overlap of the tubes at the joints. A minimum of 8 inches is recommended. This was accomplished by the addition of a 1/2-inch brass sleeve approximately 6 inches from the 1-1/2-inch sleeve.

During the investigation of the telescopic tubes under simulated remote control conditions, it was observed that binding at the joints led to adverse pressure conditions in the pipe systems. To break the bind it was necessary to increase the pressure sometimes three fold over the maximum operating pressure of 15 psi. When the joint was freed, the momentum imparted to the smaller size tubes because the excess pressure buildup was difficult to control in order that damaging impact at the joints could be prevented. As found during tests, complete destruction of a joint is possible.

As previously mentioned, the use of aluminum tubes in brine solution is not desirable because of the chemical reaction between metal and brine. A commercial lubricant under the brand name of Never-Seez was applied to the tubes. It was found to be far superior to any of the silicone or other types of lubricant previously used. It is a lubricant which contains very finely divided particles in a special hydrocarbon carrier. When placed on a metal surface, the protective film cannot be burned off or completely removed by abrasion. The film is resistant to corrosive and caustic solutions, which include dilute hydrochloric, sulphuric and nitric acid. A lubricant by the same manufacturer under the brand name of Never-See Compound Nickel special is recommended for extremely corrosive environments. The lubricant is easy to apply and is relatively economical requiring one to two cans per set of nested tubes of 1-inch to 4-inch diameter range.

D. DESIGN RECOMMENDATIONS

On the basis of the results of this investigation, of telescopic tube joints, the following design recommendations should be considered:

1. The design joint shown in Plates 2 and 3 will provide a telescopic tube that will extend or contract for working pressures to 15 psi.

2. To minimize binding, the telescopic tubes should be kept in as nearly a horizontal position as possible.
3. The tube overlap at each joint should not be less than 8 inches.
4. Aluminum sleeves should be used in lieu of brass sleeves on aluminum tubing because of the difficulty of welding brass to aluminum.
5. Teflon bushings offer less resistance than metal bushings, but are not recommended because of the difficulty of bonding them to the tube surface.
6. To minimize stress at the joints, all tube surfaces should be coated with a lubricant resistant to corrosive environments.
7. Leakage at the joint can easily be controlled by means of rubber O-rings placed on the guide sleeves.
8. A pressure control valve on the discharge side of the pump is essential for the protection against sudden excessive impact stress on the joints during mining operations.
9. During normal mining operations, the pressure head on the discharge side of the pump should not exceed 15 psi.

III. HEAD LOSS IN TELESCOPIC TUBES

A. THEORY

Flow in a circular tube is caused by a difference in energy along the tube, the flow occurring from high energy to low energy. In horizontal tubes, since potential energy and kinetic energy remain fixed, the flow occurs at the expense of the pressure intensity. In inclined or vertical tube, both potential and pressure energies change. When the cross-sectional area of the conduit changes such as at a telescopic joint, then kinetic energy may also be used to overcome friction. Whenever there is flow of a real fluid with one layer moving relative to an adjacent layer, there is internal friction (viscosity) which converts part of the flow energy into heat. Dimensionally, this loss can also be considered as the friction head loss, h_f . By applying Bernoulli's theorem between points for which the total energy is known and including any loss of energy due to friction, the following equation is obtained.

$$\frac{v_1^2}{2g} + \frac{p_1}{\gamma} + z_1 = \frac{v_2^2}{2g} + \frac{p_2}{\gamma} + z_2 + h_c + h_f \quad (18)$$

in which $V^2/2g$ is the velocity head, p/γ is the pressure head, z is the potential head referenced to an arbitrary horizontal datum,

h_c is the energy loss at the tube joint, and h_f is the friction loss. Equation 1 is strictly valid only for steady flow. However, the case of a sudden contraction is one in which the momentum equation may be applied together with the Bernoulli equation to obtain an expression for energy loss h_c in terms of velocities. In Figure 15 the sudden contraction is shown to take place between sections 1 and 2. For the given boundary geometry, the process of converting pressure energy into velocity energy is very efficient; hence, the loss from section 1 to the vena contracta, section 0, is small compared to the loss from section 0 to section 2, where kinetic energy is being reconverted into pressure energy.

Taking the fluid between sections 0 and 2 as a free body (Figure 15b) and neglecting the small shear force exerted on the walls between the two section, the momentum equation

$$\Sigma F_x = \frac{Q\gamma}{g} (V_{x_2} - V_{x_0}) \quad (19)$$

yields

$$p_0 A_2 - p_2 A_2 = \frac{Q\gamma}{g} (V_2 - V_0) \quad (20)$$

The Bernoulli equation, written between sections 0 and 2 , with the loss term h_c is

$$\frac{V_o^2}{2g} + \frac{p_o}{\gamma} = \frac{V_2^2}{2g} + \frac{p_2}{\gamma} + h_c \quad (21)$$

Solving for $(p_o - p_2)/\gamma$ in each equation and equating,

$$\frac{p_o - p_2}{\gamma} = \frac{Q}{A_2 g} (V_2 - V_o) = \frac{V_2^2 - V_o^2}{2g} + h_c \quad (22)$$

As $Q/A_2 = V_2$,

$$h_c = \frac{2V_2 (V_2 - V_o)}{2g} - \frac{V_2^2 - V_o^2}{2g} = \frac{(V_o - V_2)^2}{2g} \quad (23)$$

Using the continuity equation $V_o C_c A_2 = V_2 A_2$, where C_c is the contraction coefficient, the loss becomes

$$h_c = \left(\frac{1}{C_c} - 1 \right)^2 \frac{V_2^2}{2g} \quad (24)$$

which may also be written

$$h_c = K_c \frac{V_2^2}{2g} \quad (25)$$

Since $V_1 A_1 = V_2 A_2$, Equation 20 may also be written as follows

$$h_c = \left[\left(\frac{D_2}{D_1} \right)^2 - 1 \right] \frac{V_2^2}{2g} \quad (26)$$

applicable also to unsteady flows whose time average is steady.

For practical application, the values of V and p in Equation 1 are taken as the average values in the particular cross-section and z is the elevation above a chosen datum.

For steady flow in circular tubes the frictional loss is determined by means of the pipe-friction formula.

$$h_f = f \frac{L}{D} \frac{V^2}{2g} \quad (27)$$

in which h_f is the head (energy) loss in foot-pounds per pound in the length of tube L of inside diameter D , for average velocity of flow V . The friction factor f is dimensionless, and must be found in a manner so that Equation 2 correctly yields the energy loss. The factor f is not constant but must depend upon velocity V , diameter D , density ρ , viscosity μ and certain characteristics of the wall roughness that are signified by ϵ , ϵ' , and m . For smooth tubes such as aluminum and stainless steel tubing would be $\epsilon = \epsilon' = \underline{m} = 0$, leaving f dependent upon the first four quantities. They can be arranged in only one way to make them dimensionless, namely, $VD\rho/\mu$, which is the Reynolds number.

The energy loss due to the telescopic joint is analagous to the phenomena attending the sudden contraction of flow as shown in Figure 15 and Plate 5 , which shows a marked drop in pressure due both to the increase in velocity and to the loss of energy in turbulence. Equation 23 shows that K_c is a function of the boundary geometry D_2/D_1 . In general, the coefficient, K_c , is determined by experiments.

B. EXPERIMENTAL INVESTIGATION

For turbulent flow through the telescopic tubes, only the friction loss h_f and the junction loss h_c were investigated experimentally. The results of the study of friction loss h_f as a function of the Reynolds number are given in Figure 16 . Likewise, the results of the study of the junction loss are given in Figure 17 . The junction loss is expressed in terms of the coefficient K_c as a function of the Reynolds number and boundary geometry D_2/D_1 .

Figure 16 shows a comparison of the experimental data with the Moody diagram. The telescopic tubes performed as a rough pipe with a mean relative roughness of $e/D = 0.015$.

C. CONCLUSIONS

The results of this investigation can be summarized as follows:

1. For friction loss h_f , the scatter of data about the curve $e/D = 0.015$ is due in a large measure to
 - (a) leakage at the joints affecting the piezometric head readings downstream of the joint
 - (b) errors in measurements readings, and
 - (c) non-uniformity of pipe roughness as a result of non-uniformity in coating the interior of the pipe with lubricant.
2. For a given Reynolds number of turbulent flow, the coefficient K_c increases with a decrease in diameter size D_2/D_1 . D_2 is the diameter of the tube downstream of the tube joint.
3. The smaller the diameter tube ratio, the larger the value of K_c .

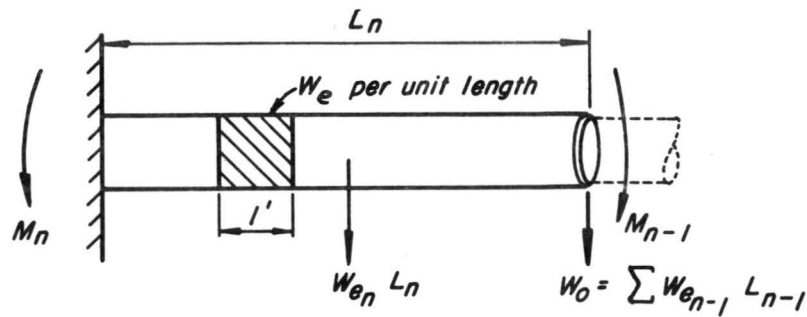


Fig. 1 Cantilever beam with effective uniform, W_e per unit of length

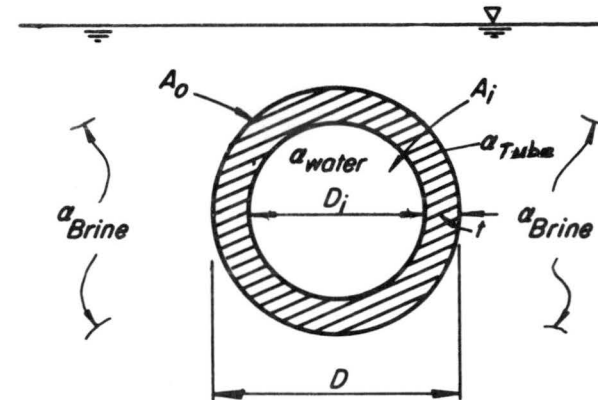


Fig. 2 Geometric characteristic of the tube with a = specific gravity

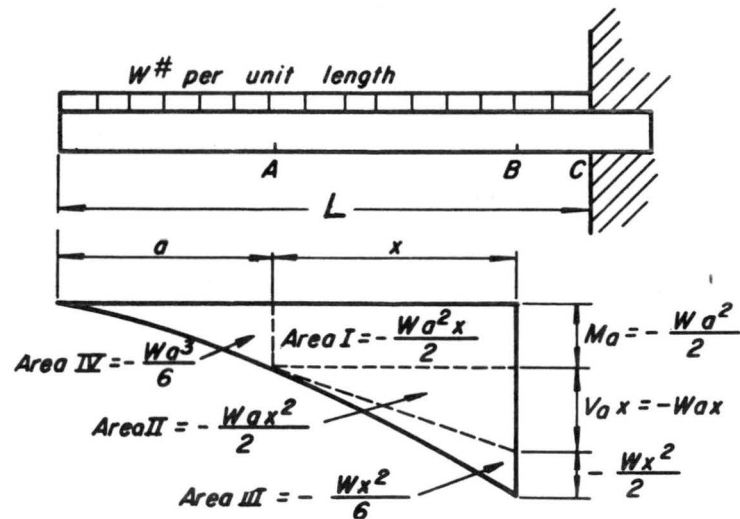


Fig. 8 Area moments for any point on a uniformly loaded cantilever beam

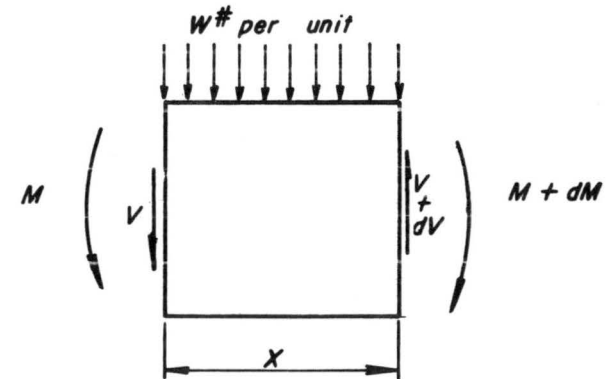


Fig. 9 Cross-section of a uniformly loaded cantilever beam

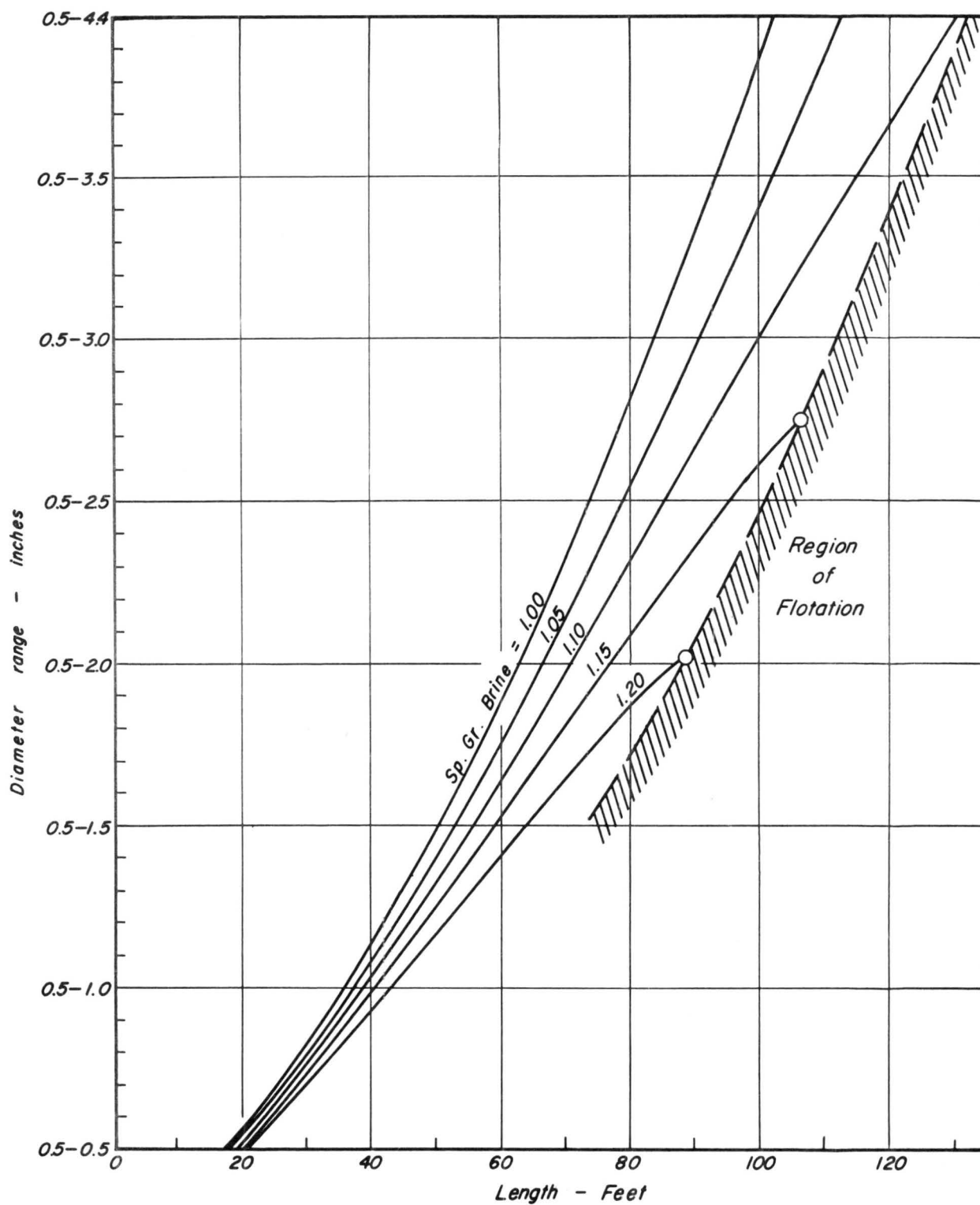


Fig. 3 Length of telescopic aluminum tube as a function of specific gravity of the salt brine (Specific gravity tube = 2.70 ; $\sigma = 14,000$ psi).

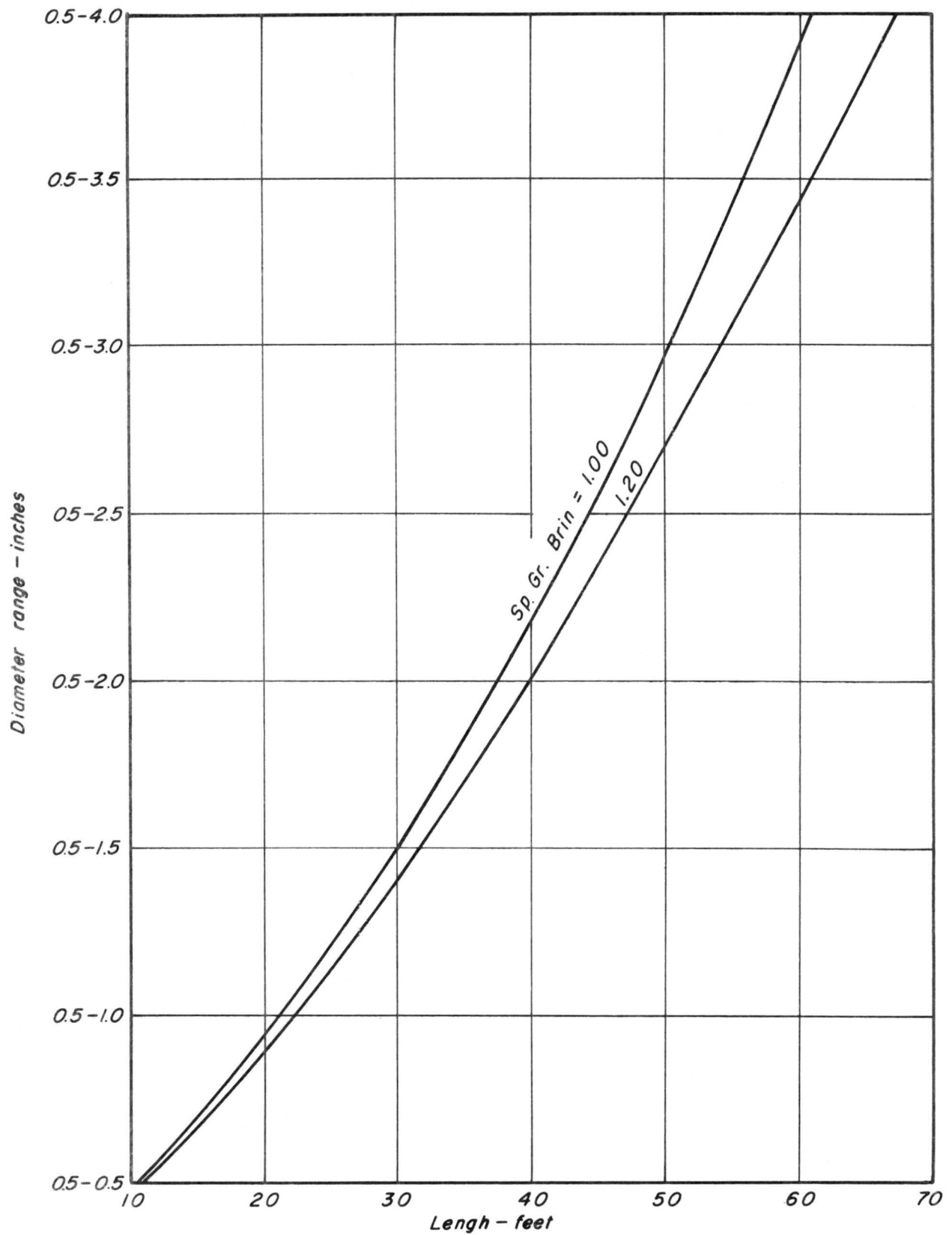


Fig. 4 Length of telescopic stainless steel tube as a function of specific gravity of the salt brine (Sp. Gr. tube = 7.80, $\sigma = 20,000$ psi)

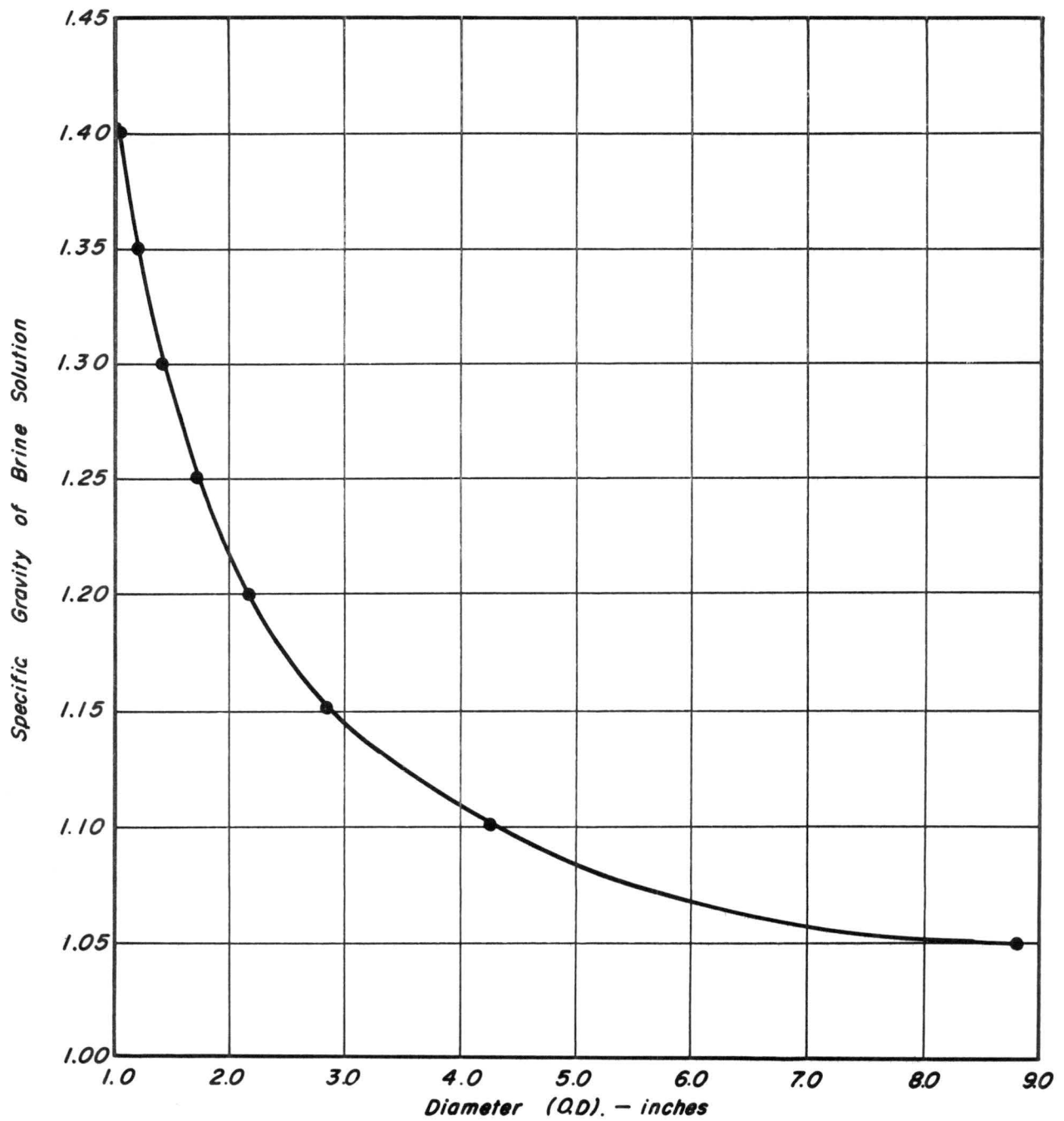


Fig. 5 Minimum diameter (O.D.) at which telescopic aluminum tubes conveying water for solution mining will float for given specific gravity of salt brine (Sp. Gr. of tube = 2.70; σ = 14,000 psi)

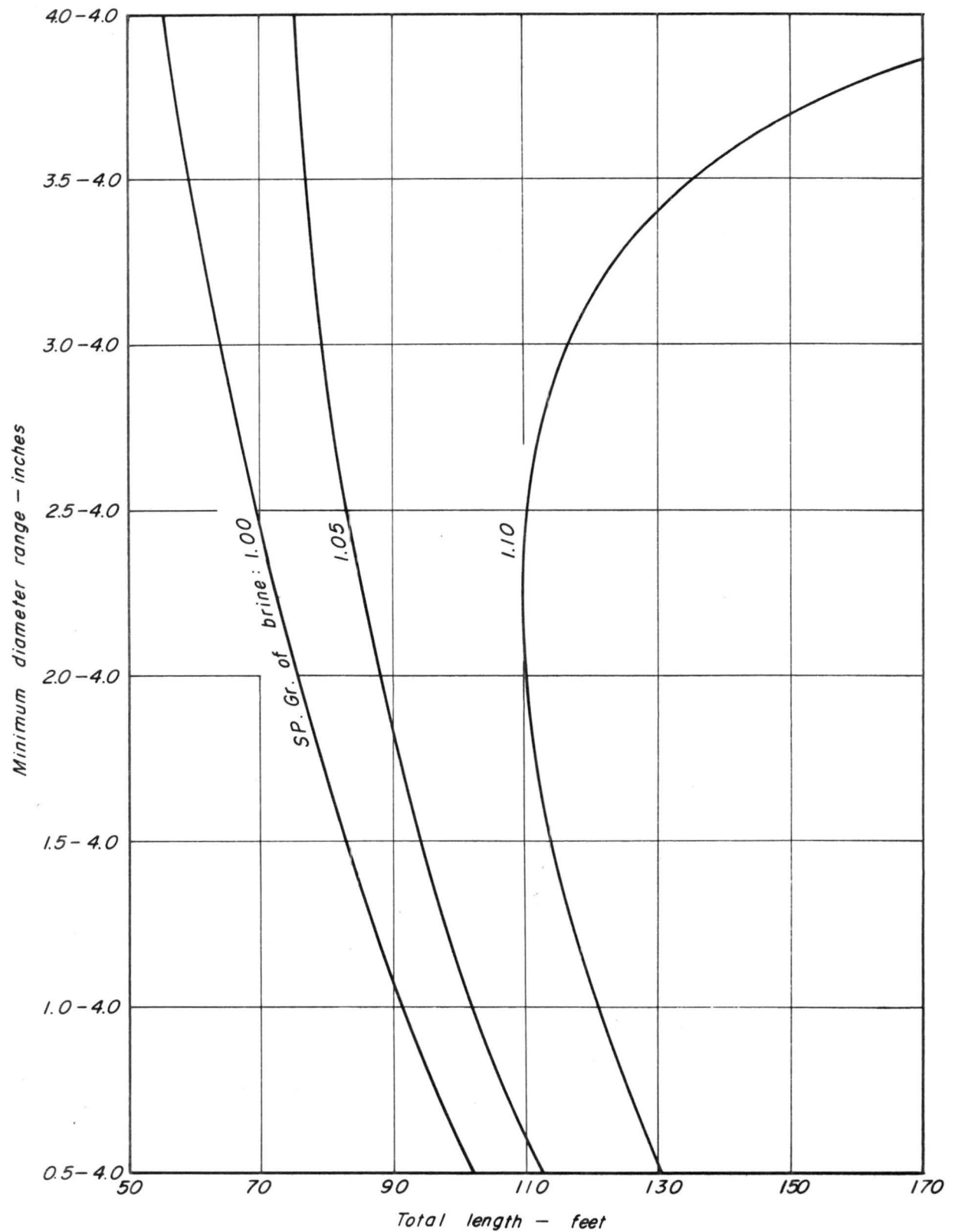


Fig. 6 Relation between minimum diameter of telescopic aluminum tubes and total length for various specific gravities of brine (Sp. Gr. tube = 2.70, $\sigma = 14,00$ psi)

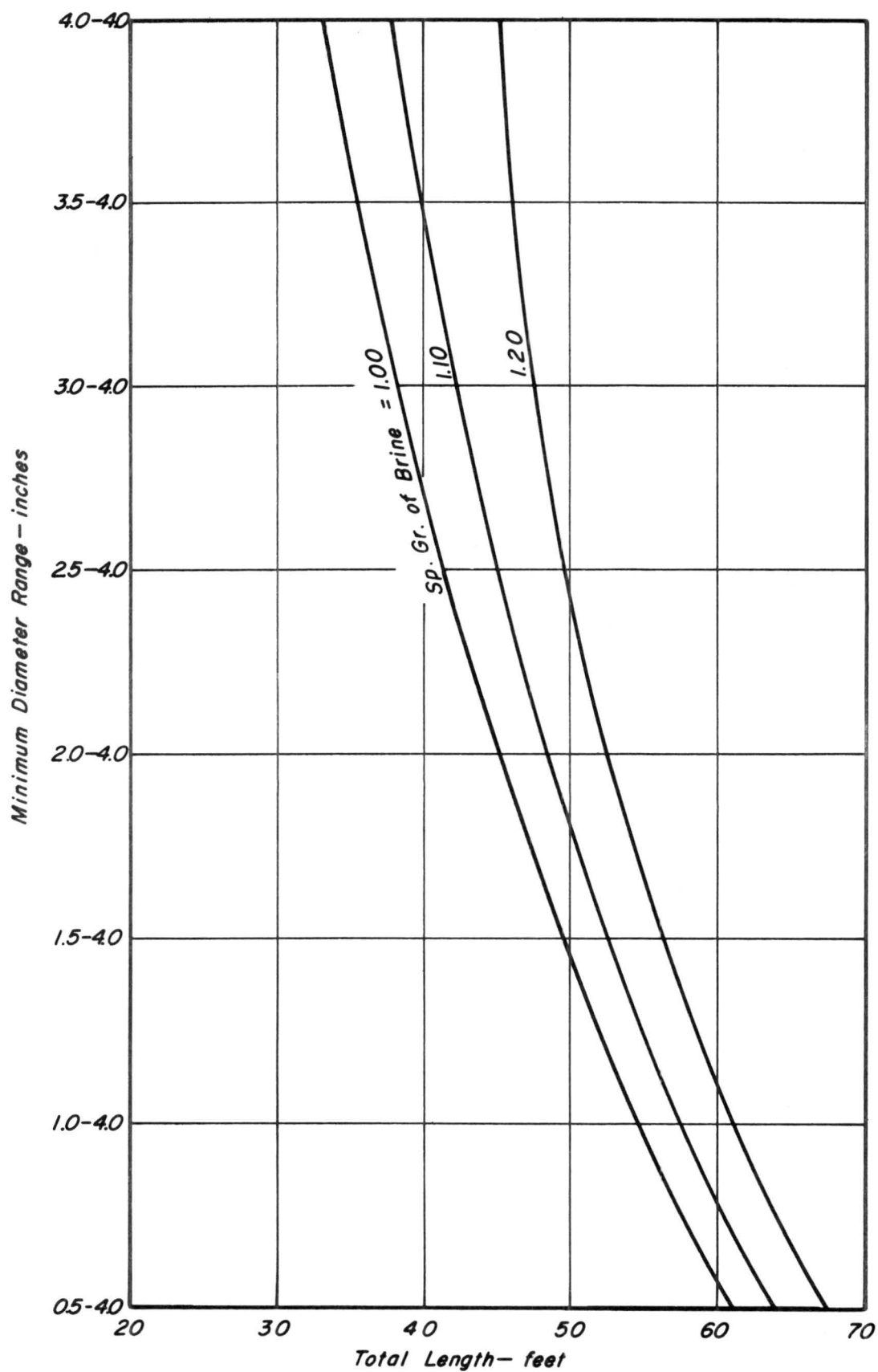


Fig. 7 Relation between minimum diameter of telescopic stainless steel tubes and total length for various specific gravities of brine (Sp. Gr. tube = 7.80, $\sigma = 20,000$ psi)

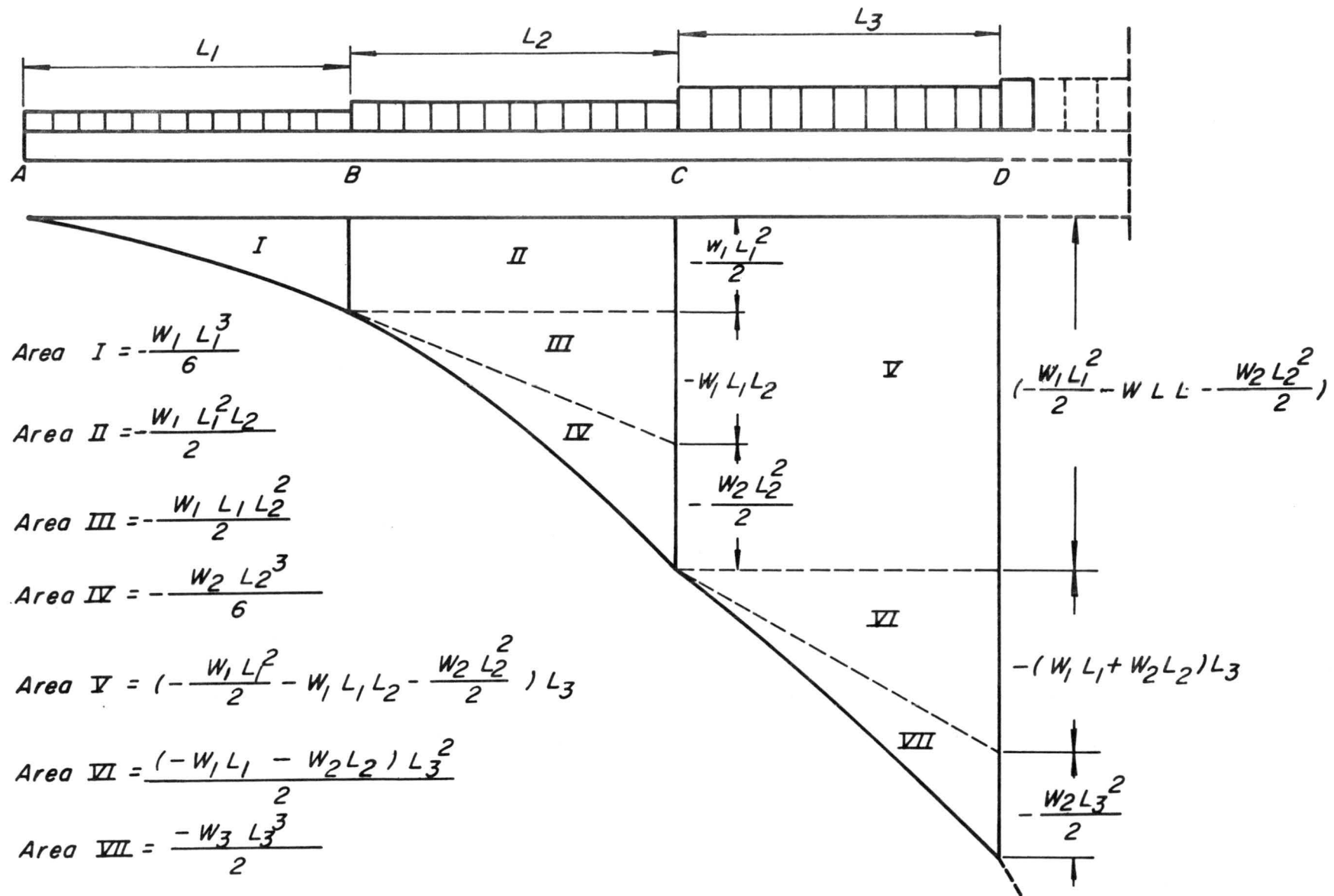


Fig. 10 Area moments for a cantilever variously loaded with w_n load per unit length

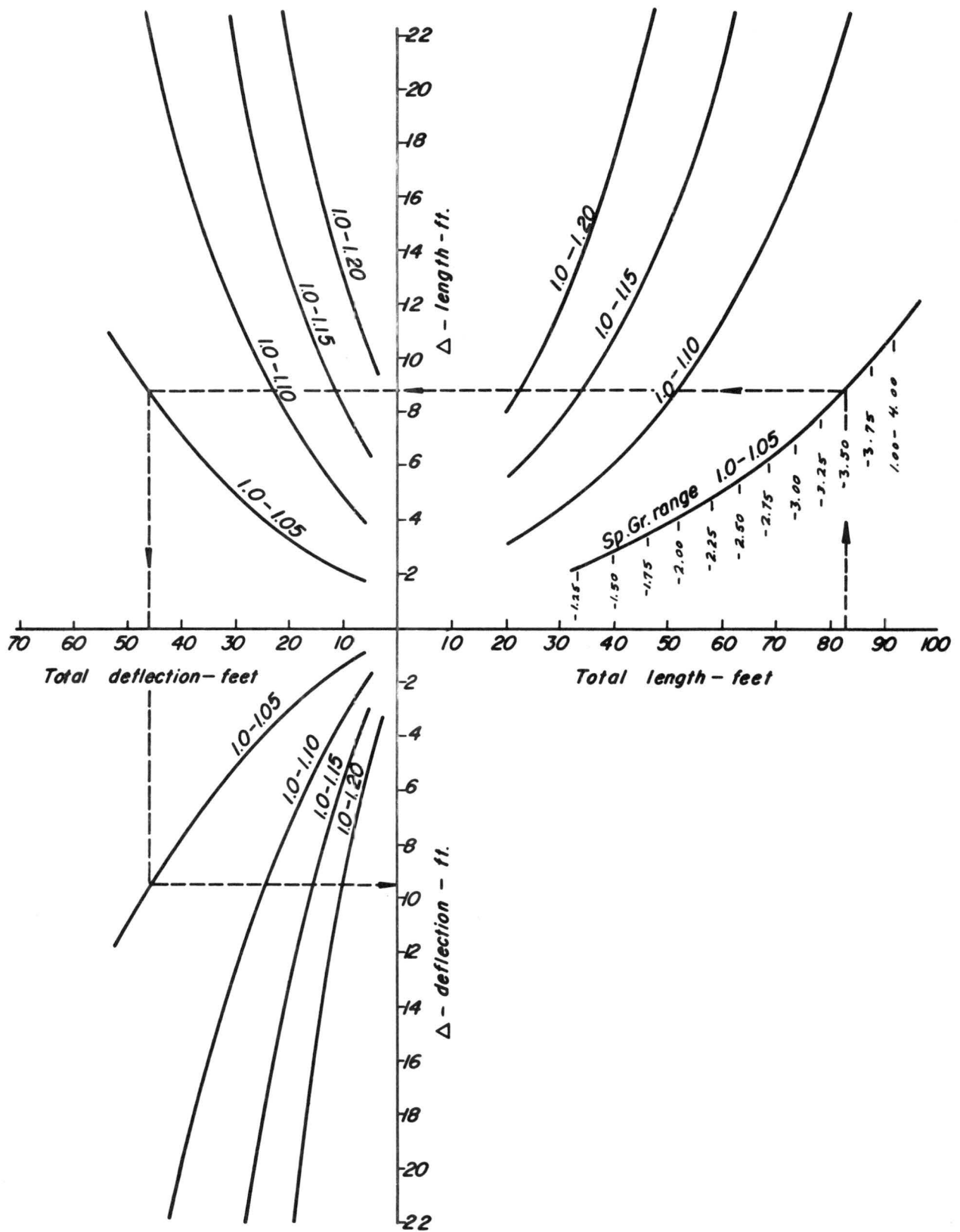


Fig. 11 Deflection of aluminum telescopic tubing for various densities of salt brine (Sp.Gr. tube = 2.70)

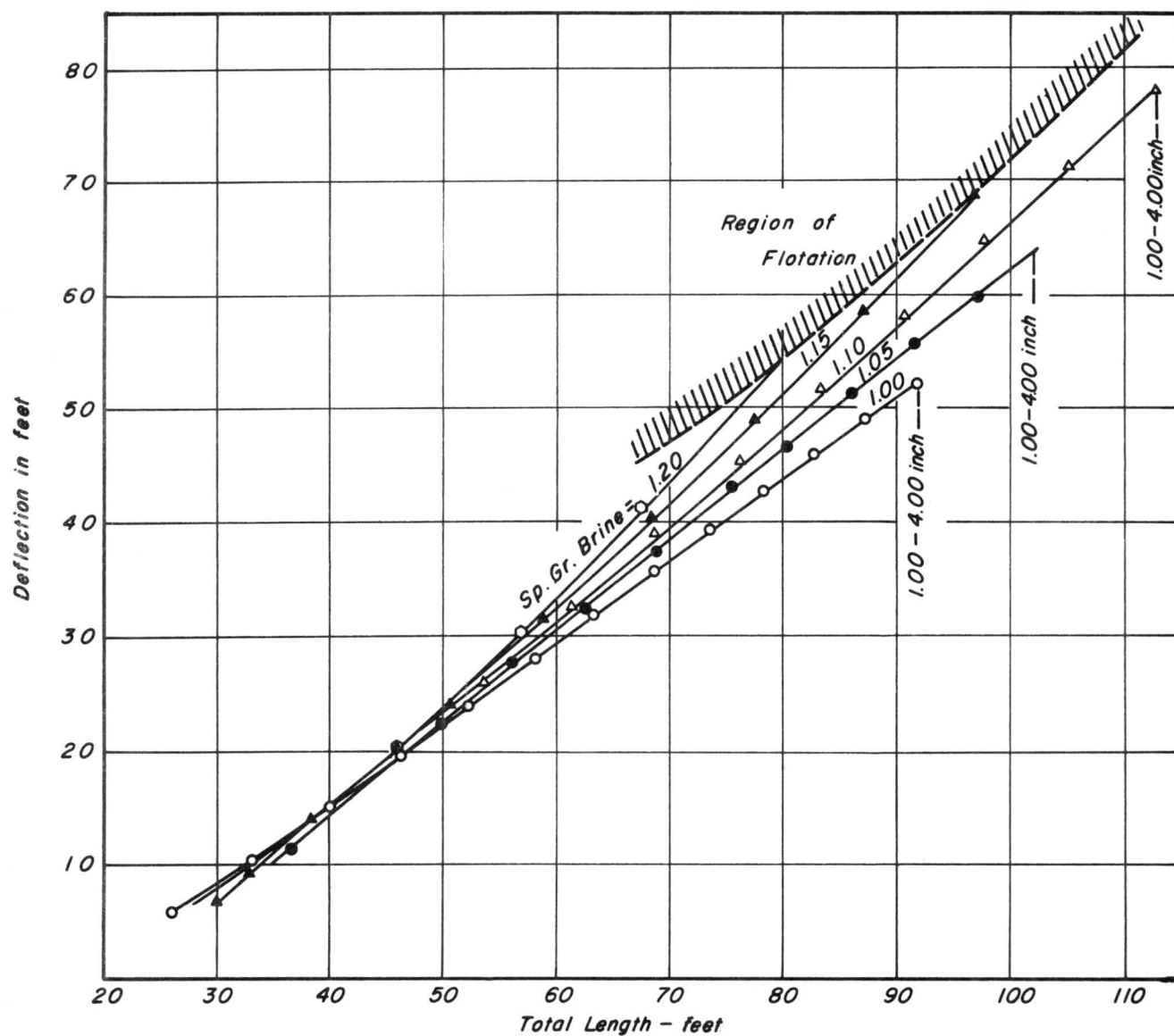


Fig. 12 Deflection for given total length of aluminum telescopic tubing for various densities of salt brine (Sp. Gr. tube = 2.70)

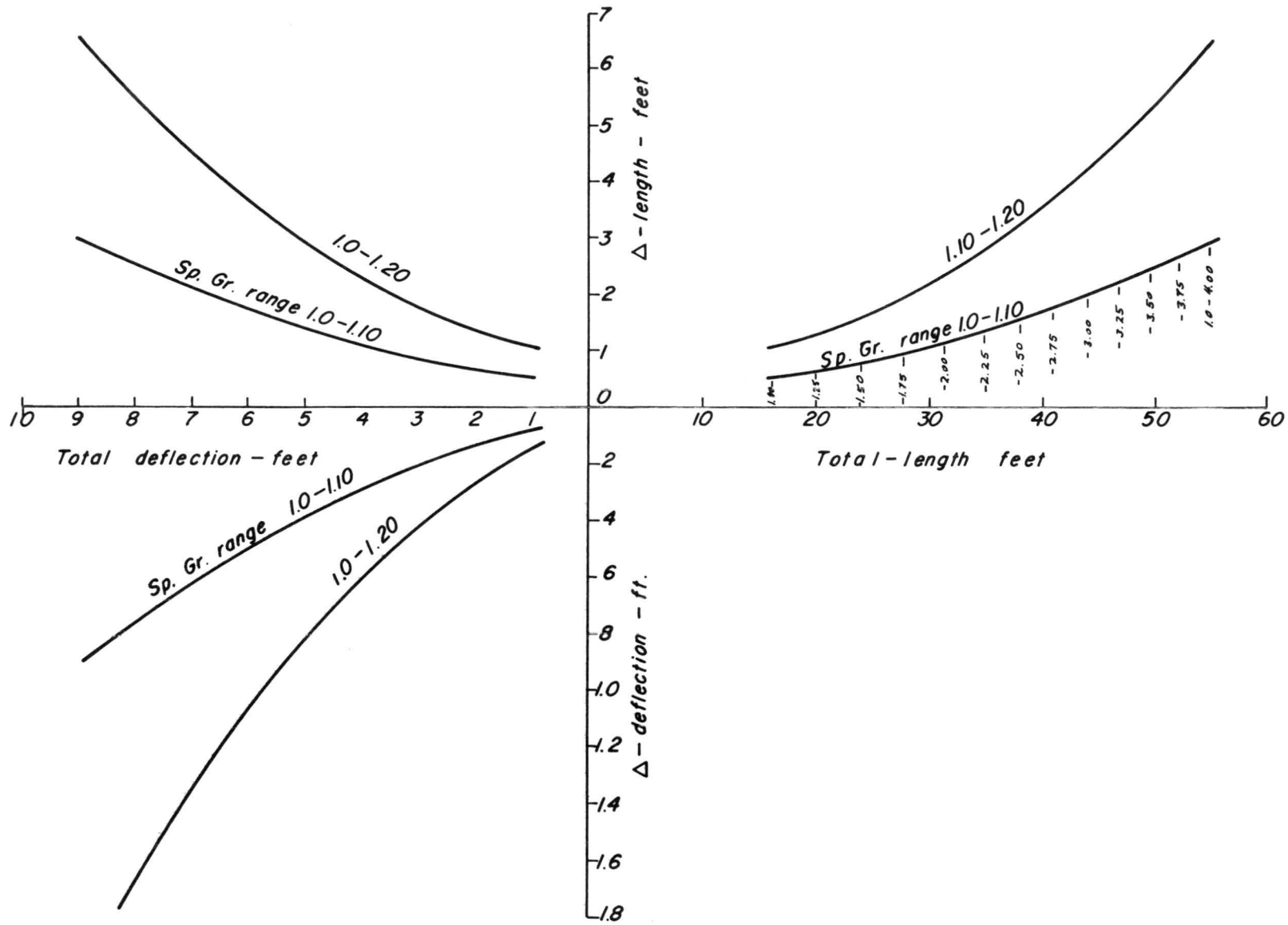


Fig. 13 Deflection of stainless steel tubing for various densities of salt brine (Sp. Gr. tube = 7.80).

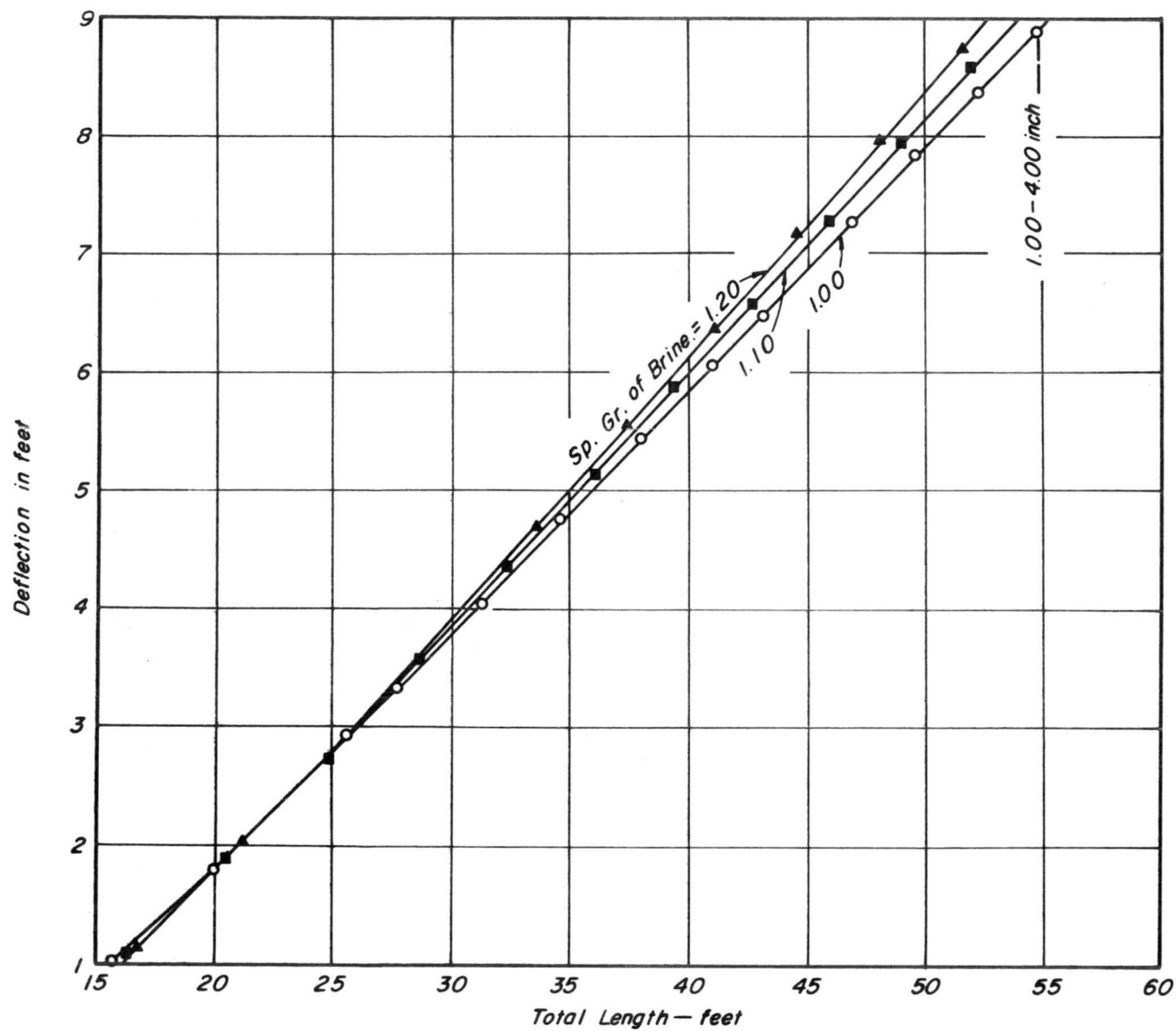
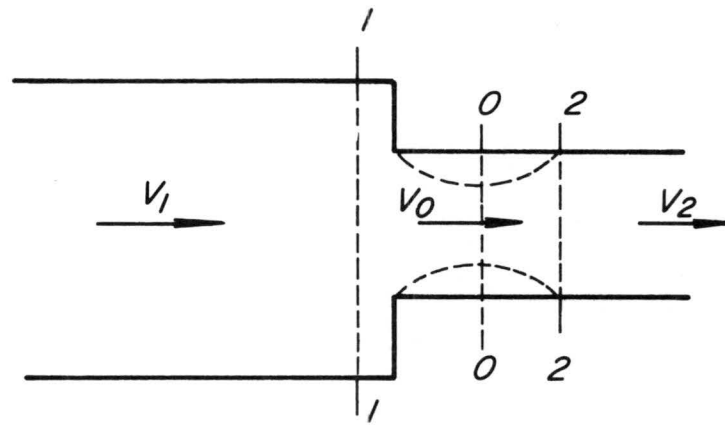
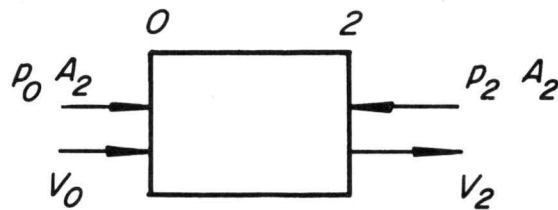


Fig. 14 Deflection for given total length of stainless steel tubing for various densities of salt brine (Sp.Gr. tube = 7.80)



(a)



(b)

Fig. 15 Sudden contraction in a pipe line

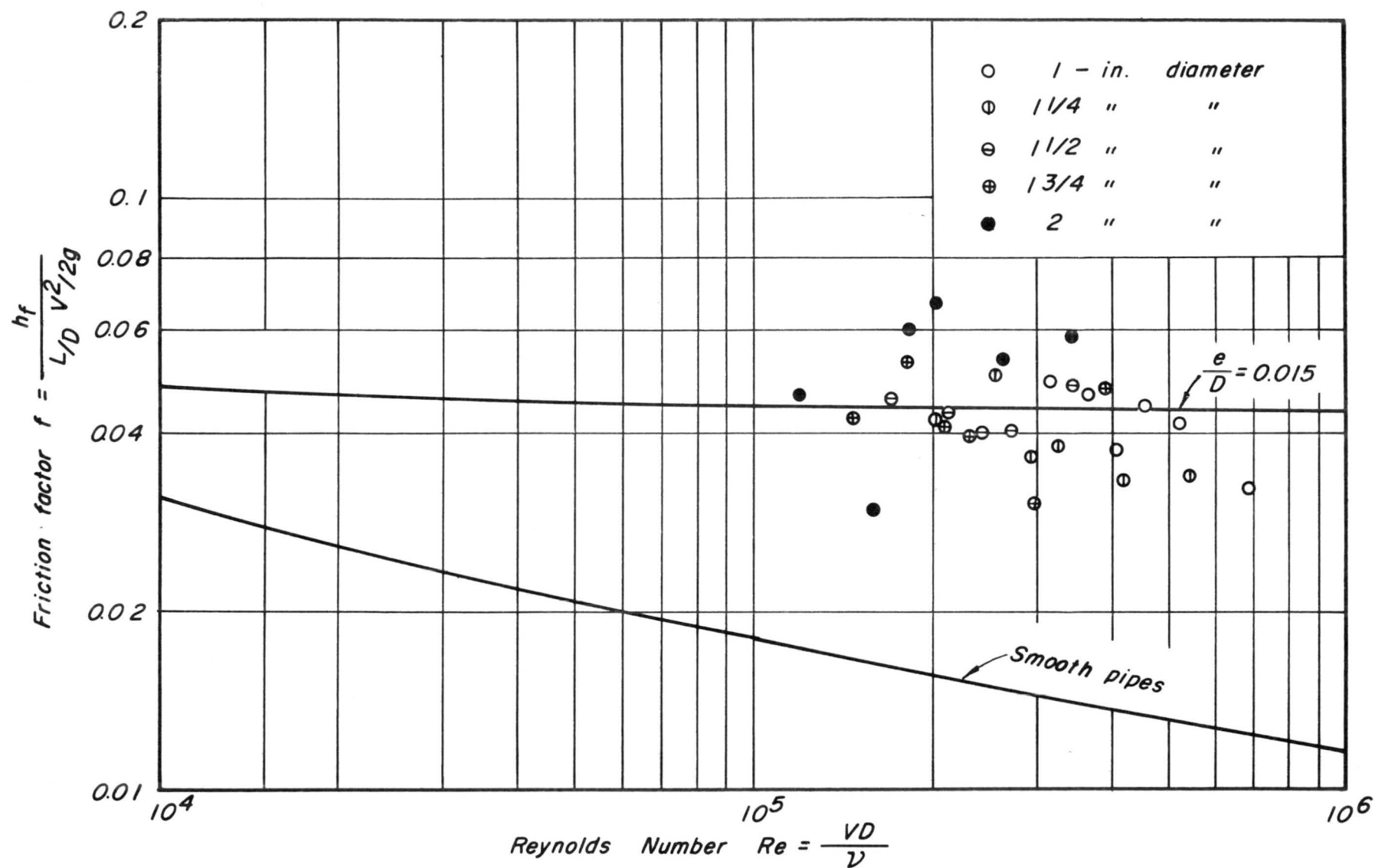


Fig. 16 Variation of resistance coefficient for uniform flow in aluminum tubes as compared with the Moody resistance diagram

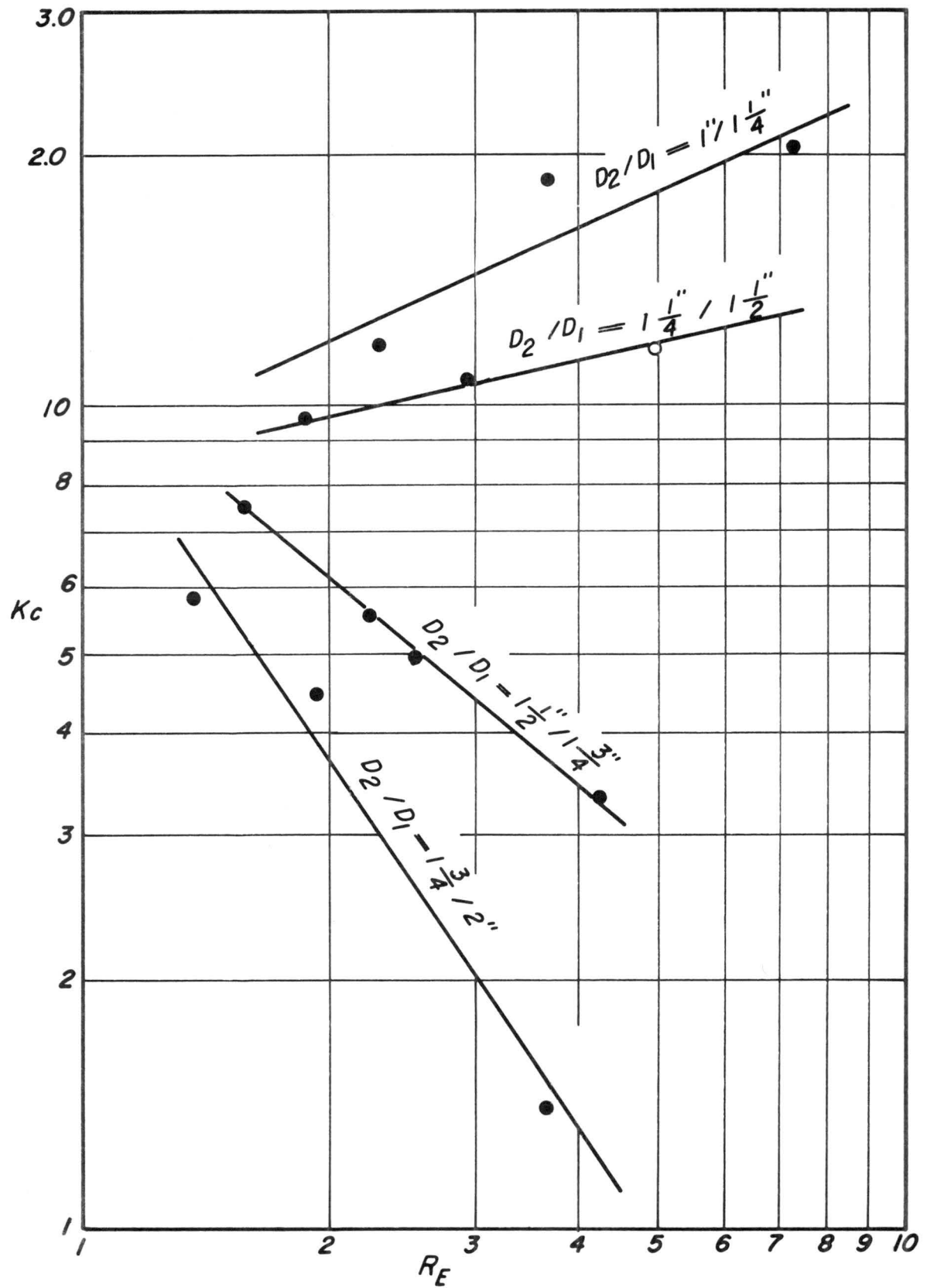
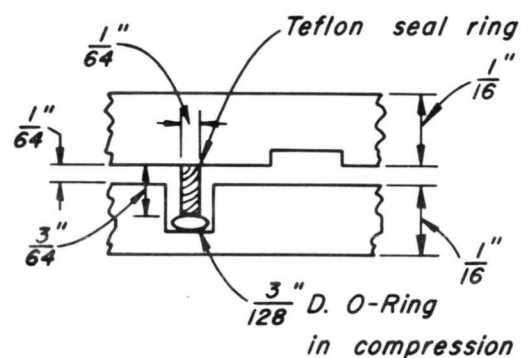
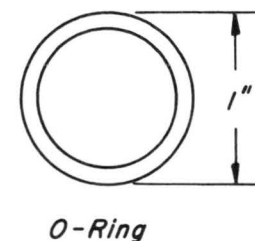
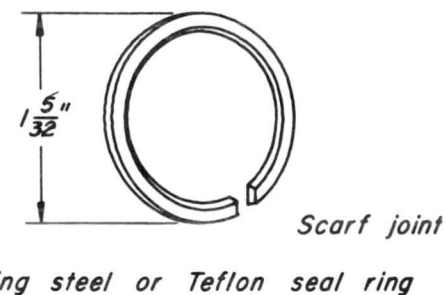
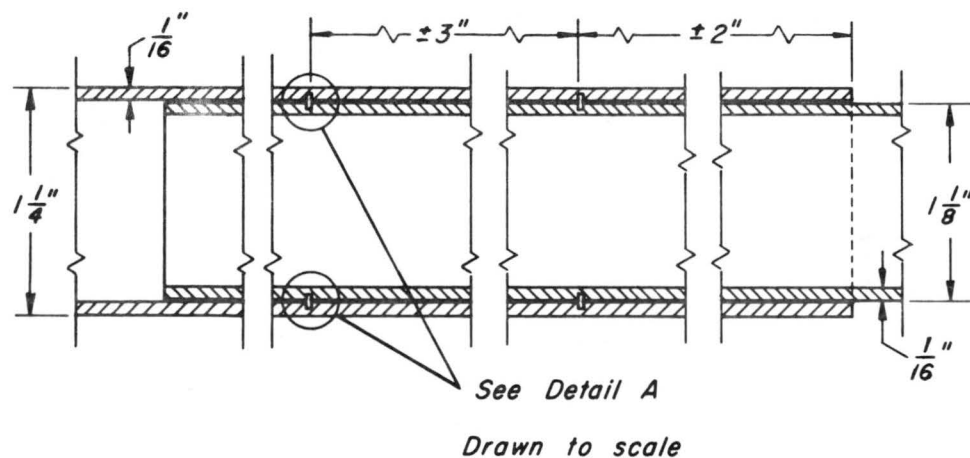
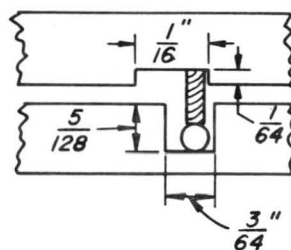


Fig. 17 Variation of telescopic joint energy loss coefficient with Reynolds number for various ratios of tube diameters.



Approach condition

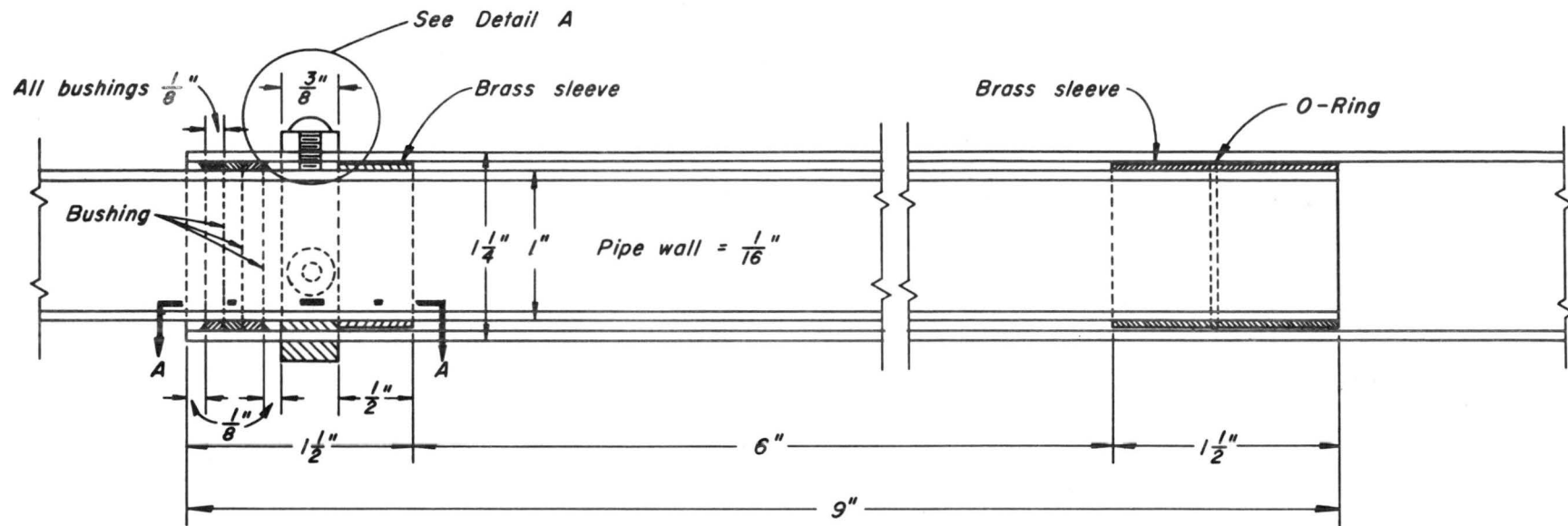


Lock position

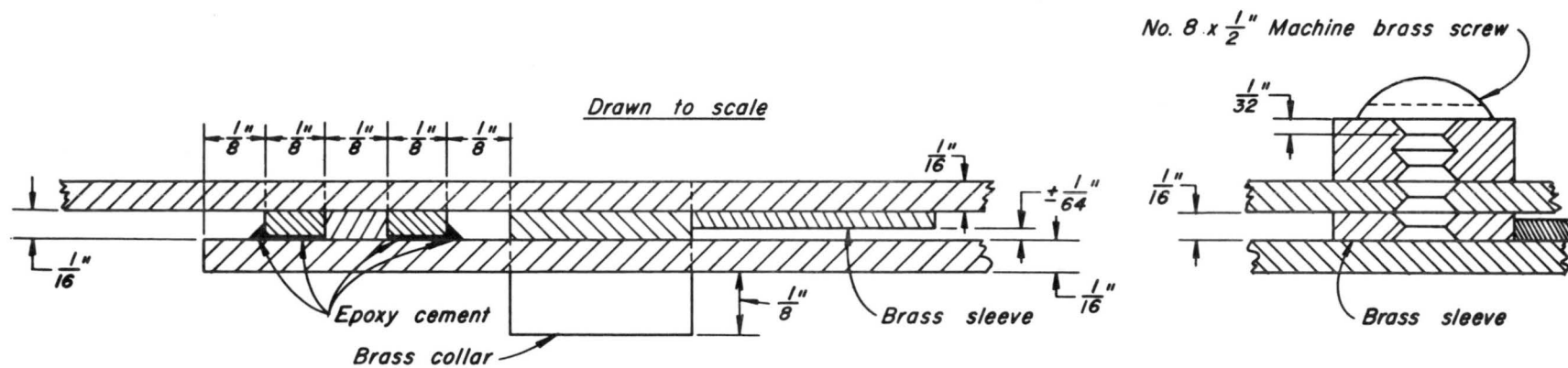
DETAIL A
 Schematic only

- NOTES:
1. Number of seal rings with O-Ring used to lock pipes in telescopic position to be determined by test.
 2. Spacing of seal rings to be determined by test.

Plate 1. Preliminary design of telescoping tube lock joint.



DETAIL OF TELESCOPIC PIPE IN LOCK POSITION



SECTION A-A

DETAIL A

Plate 2 Final design of telescoping tube slip joint showing details of joint with all tubes in extended position.

NOTES: 1. All five sections of aluminum tubes were 12'-0" in length.

2. Sections 3, 4, and 5 were identical to section 2 except for dimensions.

3. All brass screws were drilled and tapped.

4. 1" D. x $\frac{3}{8}$ " x $\frac{1}{16}$ " brass ring held in position by screws is the bearing surface for the $\frac{1}{2}$ " sleeve.

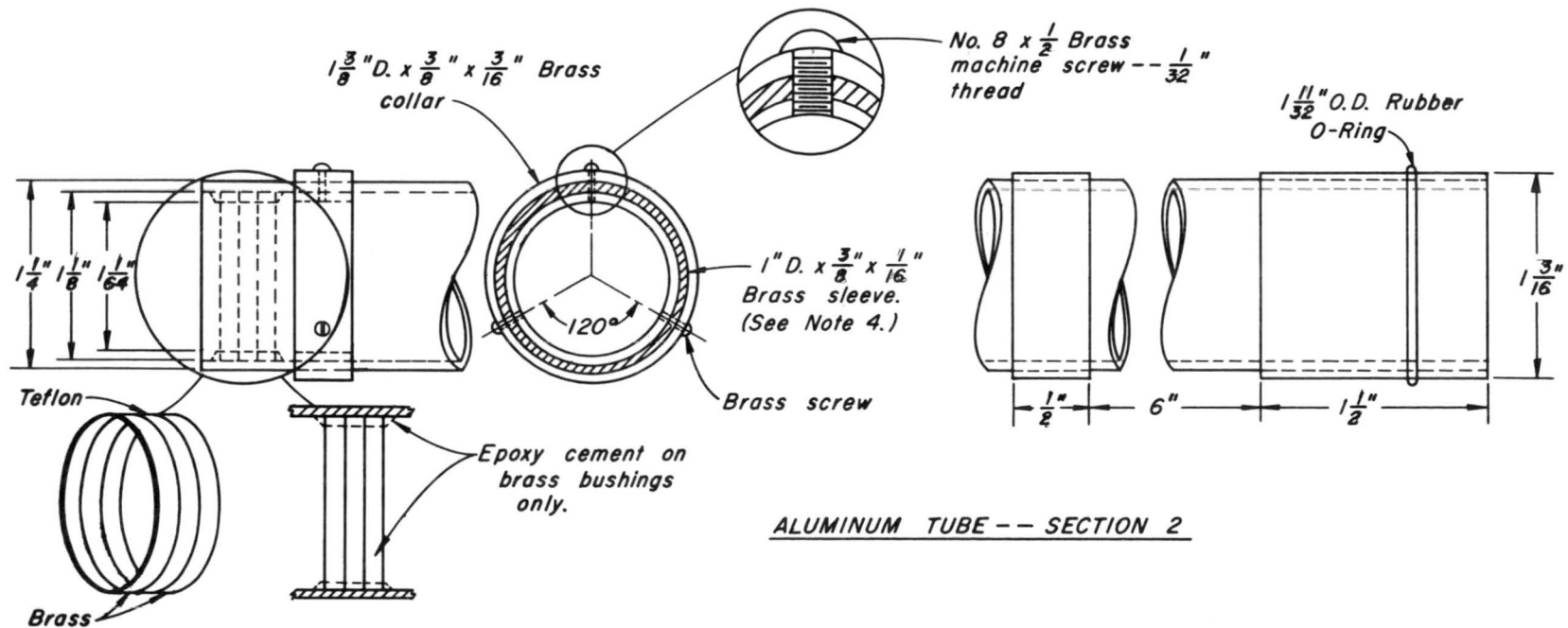
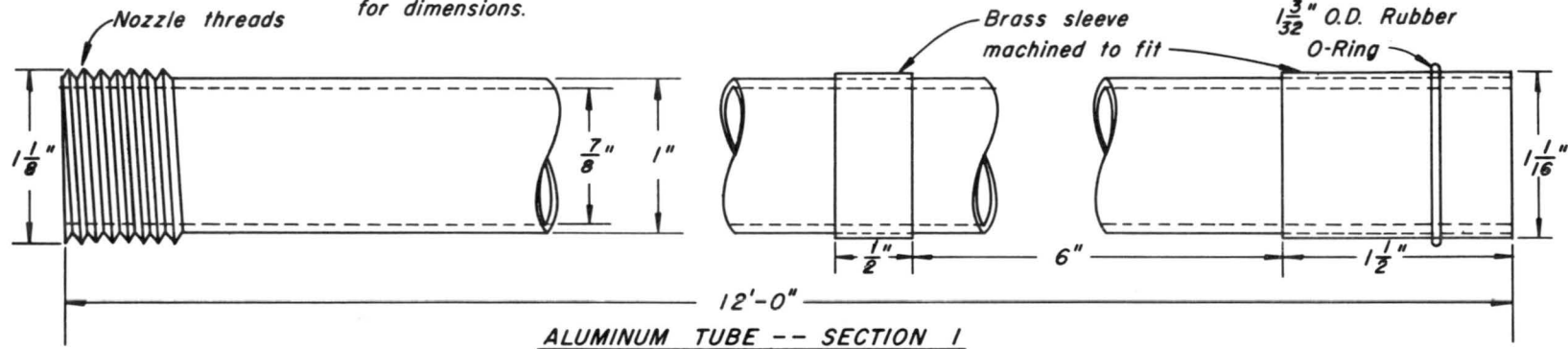
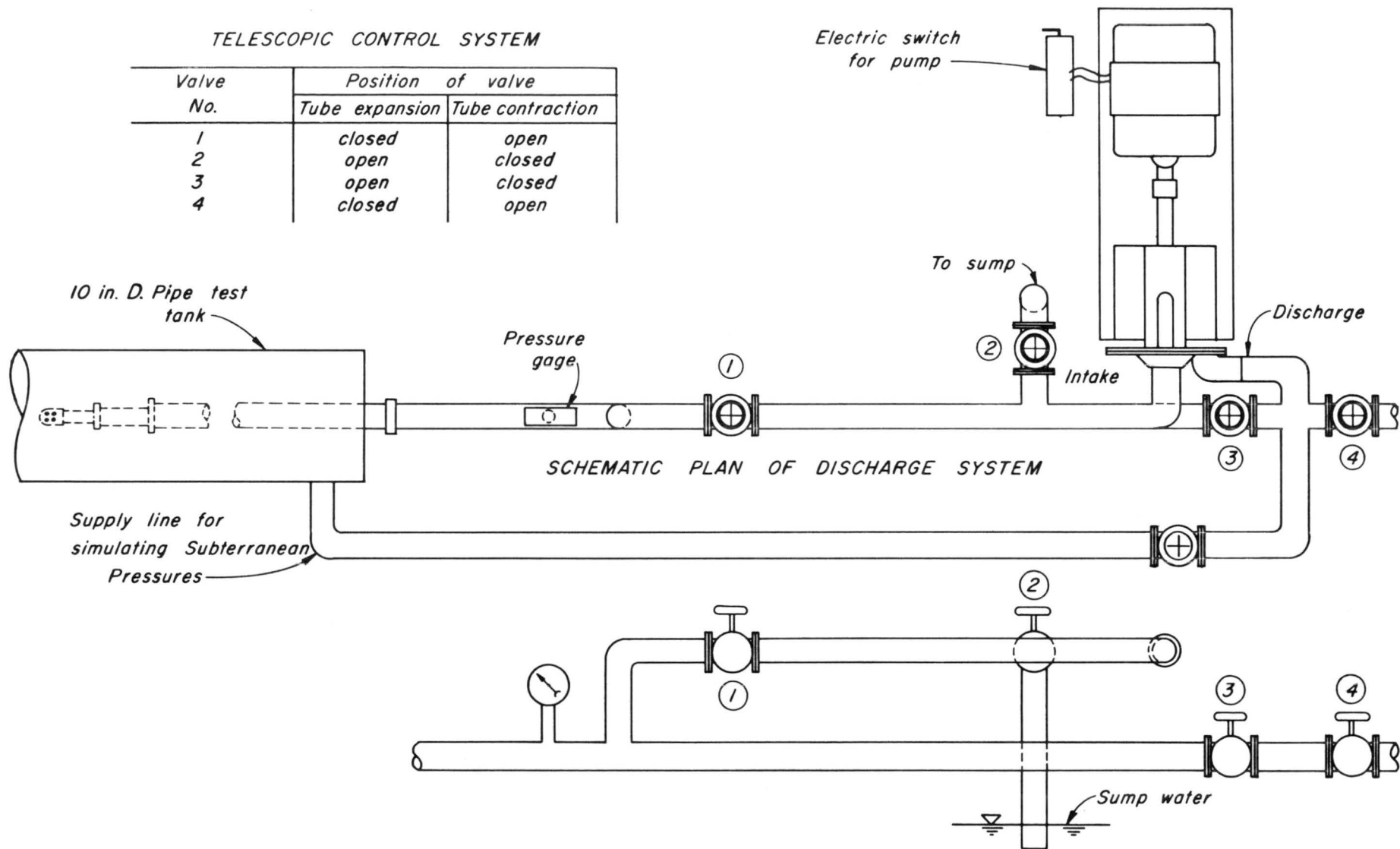


Plate 3. Details of telescoping tube slip joint not shown in Plate 2.

TELESCOPIC CONTROL SYSTEM

Valve No.	Position of valve	
	Tube expansion	Tube contraction
1	closed	open
2	open	closed
3	open	closed
4	closed	open



SCHEMATIC PLAN OF DISCHARGE SYSTEM

SCHEMATIC PROFILE OF DISCHARGE PIPE SYSTEM ONLY

Plate 4. Discharge system for extension or contraction of telescopic tubes.

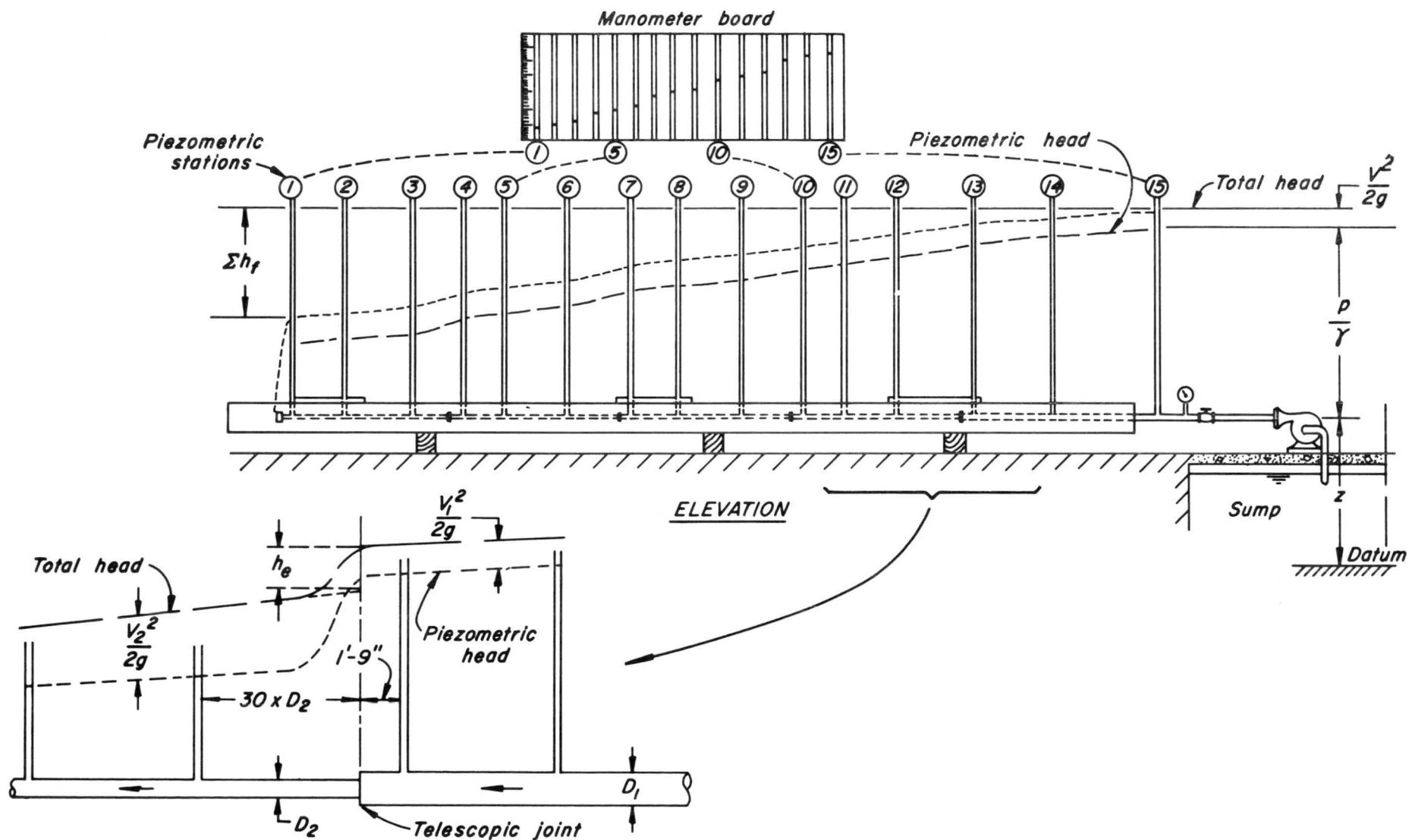


Plate 5. Schematic view showing various energy lines and method of determining head loss along the telescopic tube and at the telescopic joints.